and 24S,25-epoxycholesterol (cholest-5-en-24S,25-epoxy-3β-ol) were purchased from Steraloids (Wilton, NH). [25,26,26,26,27,27,27-$^2H_7$]4β-hydroxycholesterol, [26,26,26,27,27,27-$^2H_6$]24-hydroxycholesterol, [27,27,27-$^2H_3$]25-hydroxycholesterol, and [26,26,26,27,27,27-$^2H_6$]24,25-epoxycholesterol were obtained from Avanti Polar Lipids (Alabaster, AL). 27-Hydroxycholesterol [(25R)-cholest-5-en-3β,26-diol], [25,26,26,26,27,27,27-$^2H_7$]27-hydroxycholesterol, and [25,26,26,26,27,27,27-$^2H_7$]7α-hydroxycholesterol were prepared as described previously (24).

Picolinic acid and 2-methyl-6-nitrobenzoic anhydride were purchased from Tokyo Kasei Kogyo (Tokyo, Japan), and 4-dimethylaminopyridine and triethylamine were obtained from Wako Pure Chemical Industries (Osaka, Japan). Additional reagents and solvents were of analytical grade.

### Sample collection

Blood samples were collected from healthy human volunteers and from a patient with cerebrotendinous xanthomatosis (CTX). After coagulation and centrifugation at 1,500 *g* for 10 min, serum samples were stored at −20°C until analysis. Informed consent was obtained from all subjects, and the experimental procedures were conducted in accordance with the ethical standards of the Helsinki Declaration. Rat liver microsomes were prepared in our previous study (25) and had been stored at −70°C until they were used in the present experiments.

### Sample preparation

[$^2H_7$]4β-hydroxycholesterol (5 ng), [$^2H_7$]7α-hydroxycholesterol (10 ng) [$^2H_6$]24-hydroxycholesterol (5 ng), [$^2H_3$]25-hydroxycholesterol (1 ng), [$^2H_7$]27-hydroxycholesterol (10 ng), and [$^2H_6$]24,25-epoxycholesterol (1 ng) as internal standards and 5 μg of butylated hydroxytoluene were added to serum (5 μl) or microsomes (1 mg protein), and saponification was carried out in 0.5 ml of 1 N ethanolic KOH at 37°C for 1 h. After the addition of 0.25 ml of distilled water, sterols were extracted twice with 1 ml of *n*-hexane, and the extract was evaporated to dryness under a stream of nitrogen. Derivatization to the picolinyl ester was performed according to our previous method (23) with minor modifications. The reagent mixture for derivatization consisted of 2-methyl-6-nitrobenzoic anhydride (100 mg), 4-dimethylaminopyridine (30 mg), picolinic acid (80 mg), pyridine (1.5 ml), and triethylamine (200 μl). The freshly prepared reagent mixture (170 μl) was added to the sterol extract, and the reaction mixture was incubated at 80°C for 60 min. After the addition of 1 ml of *n*-hexane, the mixture was vortexed for 30 s and centrifuged at 700 *g* for 3 min. The clear supernatant was collected and evaporated at 80°C under nitrogen. The residue was redissolved in 50 μl of acetonitrile, and an aliquot (1 μl) was injected into the following LC-MS/MS system.

### LC-MS/MS analysis

The LC-MS/MS system consisted of a TSQ Quantum Ultra quadrupole mass spectrometer (Thermo Fisher Scientific, San Jose, CA) equipped with an H-ESI probe and a Nanospace SI-2 HPLC system (Shiseido, Tokyo, Japan). Chromatographic separation was performed using a Hypersil GOLD column (150 × 2.1 mm, 3 μm, Thermo Electron) at 40°C, and the following gradient system was used at a flow rate of 300 μl/min: initially, the mobile phase was composed of acetonitrile-methanol-water (40:40:20, v/v/v) containing 0.1% acetic acid; then it was programmed in a linear manner to acetonitrile-methanol-water (45:45:10, v/v/v) containing 0.1% acetic acid over 20 min. The final mobile phase was kept constant for an additional 20 min.

The general LC-MS/MS conditions were as follows: spray voltage, 1,000 V; vaporizer temperature, 350°C; sheath gas (nitrogen) pressure, 85 psi; auxiliary gas (nitrogen) flow, 60 arbitrary units; ion transfer capillary temperature, 350°C; collision gas (argon) pressure, 1.5 mTorr; and ion polarity, positive. Selected reaction monitoring (SRM) was conducted using the characteristic precursor-to-product ion transition under optimized collision energy, as listed in **Table 1**.

### Statistics

Data are reported as the mean ± SD. Reproducibility was analyzed by one-way layout (JMP software; SAS Institute Inc., Cary, NC). Recovery was analyzed using a polynomial equation (26). Linearity of the calibration curves was analyzed by simple linear regression. Regression analysis was also used to calculate the estimated amount ±95% confidence limit in the recovery study. For all analyses, significance was accepted at the level of $P < 0.05$.

## RESULTS

### Selection of monitoring ions for SRM

Seven oxysterols were converted into the corresponding picolinyl ester derivatives and positive ESI-MS, MS/MS,

TABLE 1. Positive ESI-MS, MS/MS, SRM, and HPLC data of the picolinoyl ester derivative of each oxysterol

| Oxysterols (Derivatives) | MS Data $[M+Na]^+$ (Relative Intensity) | MS/MS Data[a] (Collision Energy at Maximum Intensity) | SRM Data[b] | | | HPLC Data[b] (RRT[d]) |
|---|---|---|---|---|---|---|
| | | | Collision Energy | Precursor to Product | S/N[c] | |
| | *m/z* (%) | *m/z* (*V*) | *V* | *m/z* | | |
| 4β-Hydroxycholesterol (cholest-5-en-3β,4β-dipicolinates) | 635 (100) | 146 (22) 512 (20) | 22 | 635 → 146 | 200 | 0.77 |
| 7α-Hydroxycholesterol (cholest-5-en-3β,7α-dipicolinates) | 635 (100) | 146 (15) –[e] | 15 | 635 → 146 | 200 | 0.62 |
| 22R-Hydroxycholesterol (cholest-5-en-3β,22R-dipicolinates) | 635 (100) | 146 (26) 512 (22) | 22 | 635 → 512 | 40 | 0.45 |
| 24S-Hydroxycholesterol (cholest-5-en-3β,24S-dipicolinates) | 635 (100) | 512 (22) 146 (31) | 22 | 635 → 512 | 80 | 0.48 |
| 25-Hydroxycholesterol (cholest-5-en-3β,25-dipicolinates) | 635 (100) | 512 (19) 146 (28) | 22 | 635 → 512 | 40 | 0.51 |
| 27-Hydroxycholesterol (cholest-5-en-3β,27-dipicolinates) | 635 (100) | 512 (12) 146 (33) | 22 | 635 → 512 | 80 | 0.56 |
| 24S,25-Epoxycholesterol (cholest-5-en-24S,25-epoxy-3β-picolinate) | 528 (100) | 146 (20) —[e] | 20 | 528 → 146 | 80 | 0.41 |

ESI, electrospray ionization; MS, mass spectrometry; MS/MS, tandem mass spectrometry; RRT, relative retention time; S/N, signal-to-noise ratio; SRM, selected reaction monitoring.

[a] $[M+Na]^+$ was used as a precursor ion for each MS/MS analysis. Major product ions were arranged in the order of abundance from left to right.

[b] The same HPLC column and flow rate described in Materials and Methods were employed.

[c] S/Ns were determined by injecting 100 fg of each derivative.

[d] RRTs are expressed relative to the retention time of cholesterol 3β-picolinate.

[e] Intense ion (>5% of base peak) was not observed.

SRM, and HPLC data were obtained for each of them (Table 1). All picolinyl ester derivatives exhibited $[M+Na]^+$ ions as the base peaks. The fragmentation pattern of the base peak ion of each derivative was examined under various levels of collision energy, and [M+Na−picolinic acid $(C_6H_5NO_2)]^+$ ($m/z$ = 512) or [picolinic acid $(C_6H_5NO_2)$+ $Na]^+$ ($m/z$ = 146) ions were observed as the most-abundant product ions, so that they were selected as monitoring ions for authentic oxysterols by SRM. The monitoring ions and optimal collision energies for deuterated internal standards were $m/z$ 642 → 146 (22 V) for 3β,4β-dipicolinates of [$^2H_7$] 4β-hydroxycholesterol, $m/z$ 642 → 146 (15 V) for 3β,7α-dipicolinates of [$^2H_7$]7α-hydroxycholesterol, $m/z$ 641 → 518 (22 V) for 3β,24-dipicolinates of [$^2H_6$]24-hydroxycholesterol, $m/z$ 638 → 515 (22 V) for 3β,25-dipicolinates of [$^2H_3$]25-hydroxycholesterol, $m/z$ 642 → 519 (22 V) for 3β,27-dipicolinates of [$^2H_7$]27-hydroxycholesterol, and $m/z$ 534 → 146 (20 V) for 3β-picolinate of [$^2H_6$]24,25-epoxycholesterol.

### Sensitivity of the present method

To determine the sensitivity of our SRM method, the standard mixture solution of the seven oxysterol derivatives was diluted and injected into the LC-MS/MS system. The limit of detection (signal-to-noise ratio of 3) of each steroid was 2 fg (5 amol) on-column for 4β-hydroxycholesterol and 7α-hydroxycholesterol, 5 fg (12.5 amol) on-column for 24S-hydroxycholesterol, 27-hydroxycholesterol, and 24S,25-epoxycholesterol, and 10 fg (25 amol) on-column for 22R-hydroxycholesterol and 25-hydroxycholesterol.

### Calibration curves

A calibration plot was established for each oxysterol. Different amounts of authentic oxysterol were mixed with deuterated internal standard, derivatized to the picolinyl ester, and quantified as described in the Materials and Methods. The weight ratio of each oxysterol, relative to the corresponding deuterated internal standard, was plotted on the abscissa, and the peak area ratio of the picolinyl ester of the authentic oxysterol to the deuterated variant measured by SRM was plotted on the ordinate. Because deuterium-labeled 22R-hydroxycholesterol was not available, [$^2H_6$]24-hydroxycholesterol was used as an internal standard for 22R-hydroxycholesterol. The linearity of the standard curves, as determined by simple linear regression, was excellent, as shown in **Table 2.**

### Representative SRM

The separation of various authentic oxysterol picolinates by SRM is shown in **Fig. 2A.** All oxysterol picolinates tested were successfully separated. 7β-Hydroxycholesterol, an autoxidation product of cholesterol, gave a peak just before 7α-hydroxycholesterol (not shown in the figure), and the retention times (relative to cholesterol) of these oxysterols (as picolinates) were 0.61 and 0.62, respectively. Figure 2B–D shows typical SRM chromatograms obtained from 1 mg of protein from rat liver microsomes (Fig. 2B) and 5 μl of sera from a control subject (Fig. 2C) and a CTX patient (Fig. 2D). In rat liver microsomes, a significant amount of 24S,25-epoxycholesterol was detected, whereas only a trace amount of 24S-hydroxycholesterol was observed. In contrast, human serum contained a very low concentration of 24S,25-epoxycholesterol, but a significant amount of 24S-hydroxycholesterol was present. When serum oxysterol profiles were compared between controls and CTX, markedly reduced serum 25- and 27-hydroxycholesterol concentrations were observed.

### Precision and accuracy of the present method

The following studies were performed to determine the precision and accuracy of the present method using rat liver microsomes. Reproducibility was investigated by analyzing four samples in triplicate by LC-MS/MS (**Table 3**). The results were analyzed by a one-way layout, in which the analytical errors were divided into two sources: sample preparation and SRM measurement. The variances were not considered to be attributable to the sample preparation, because the errors during sample preparation were not significantly larger than those between the measurements (see supplementary Tables I, II). The inter-assay coefficients of variation for the between- and within-sample variations were 1.8% to 12.7% and 2.9% to 11.9%, respectively.

For the recovery experiment, known amounts of oxysterols (a, 2a, 3a; a = 0.05–4.0 ng) were spiked into 1 mg of rat liver microsomal protein (n = 2). After alkaline hydrolysis and derivatization, LC-MS/MS was carried out in triplicate for each sample. The recoveries of the known spiked amounts of the oxysterols ranged from 86.7% to 107.3%, with a mean of 100.6% (**Table 4**). In addition, the amounts of each endogenous oxysterol found in 1 mg of unspiked microsomal protein were within the 95% confidence limit for the estimated amount of each

TABLE 2. Linearities of calibration plots for each oxysterol

| Oxysterol | Range (n) | Linear Regression Equation[a] | Correlation Coefficient ($r$) |
|---|---|---|---|
| | *ng* | | |
| 4β-Hydroxycholesterol | 0.05 – 10 (7) | $Y = 0.436X - 0.009$ | 0.999 |
| 7α-Hydroxycholesterol | 0.1 – 20 (7) | $Y = 1.075X - 0.011$ | 1.000 |
| 22R-Hydroxycholesterol | 0.05 – 5 (6) | $Y = 0.084X - 0.000$ | 0.993 |
| 24S-Hydroxycholesterol | 0.05 – 5 (6) | $Y = 0.615X - 0.010$ | 0.996 |
| 25-Hydroxycholesterol | 0.01 – 1 (6) | $Y = 0.935X - 0.007$ | 1.000 |
| 27-Hydroxycholesterol | 0.1 – 10 (6) | $Y = 1.400X - 0.020$ | 0.998 |
| 24S,25-Epoxycholesterol | 0.01 – 2 (7) | $Y = 0.444X - 0.004$ | 0.998 |

[a] $X$ is the weight ratio of each oxysterol to the corresponding deuterated internal standard, and $Y$ is the peak area ratio calculated as the peak area of the oxysterol-picolinate(s) divided by that of deuterated oxysterol-picolinate(s) (internal standard). [$^2H_6$]24-hydroxycholesterol was used as an internal standard for 22R-hydroxycholesterol.

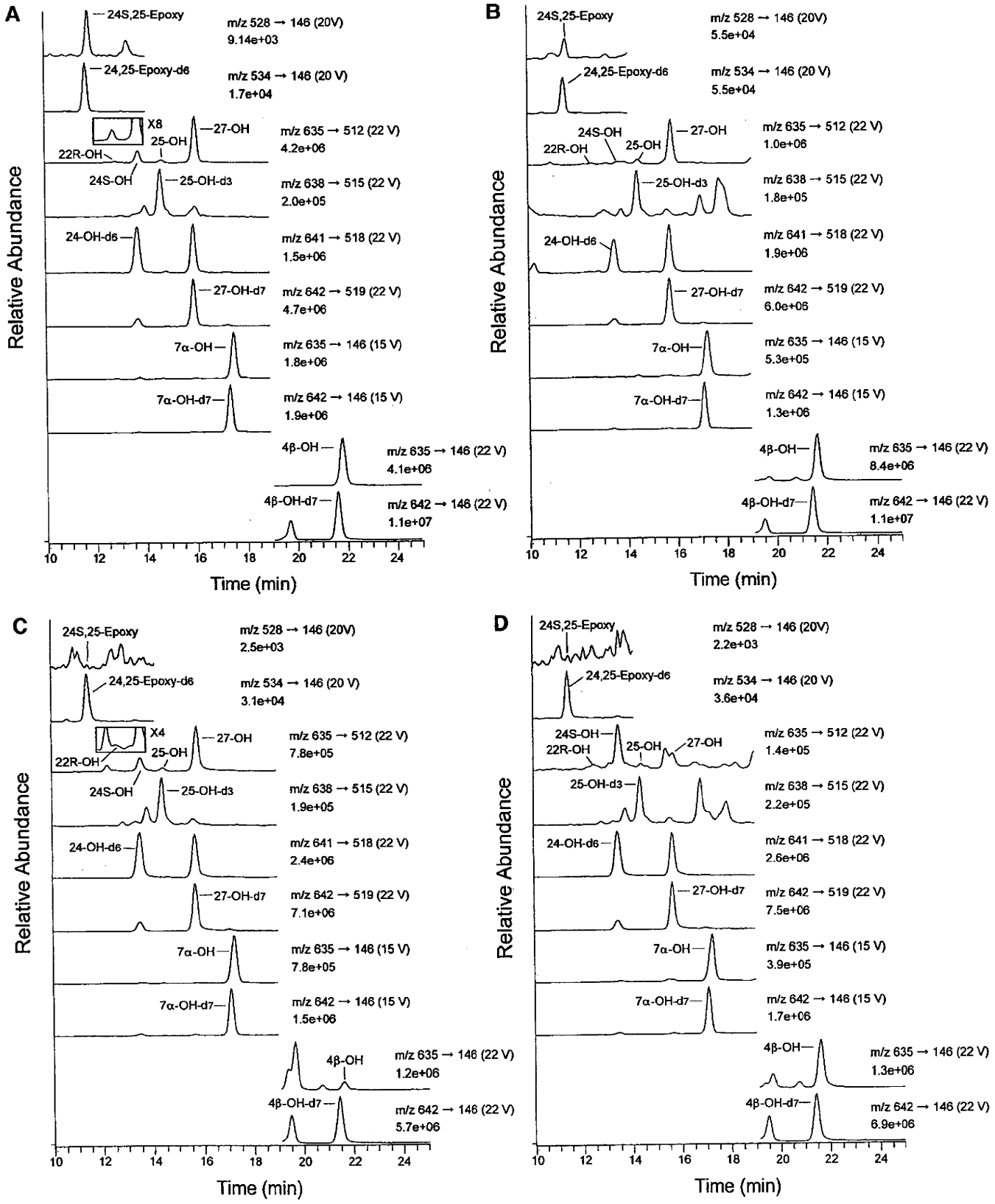


**Fig. 2.** Comparison of selected reaction monitoring chromatograms obtained from authentic oxysterols (A), 1 mg protein of the microsomal fraction from a normal rat liver (B), and 5 μl of sera from a normal volunteer (C) and a patient with CTX (D). The quantities of each peak (in A) of authentic oxysterol standards are: ~200 pg for 7α-hydroxycholesterol (7α-OH), [$^2H_7$]7α-OH (7α-OH-$d_7$), 27-hydroxycholesterol (27-OH), and [$^2H_7$]27-OH (27-OH-$d_7$), ~100 pg for 4β-hydroxycholesterol (4β-OH), [$^2H_7$]4β-OH (4β-OH-$d_7$), 24S-hydroxycholesterol (24S-OH), and [$^2H_6$]24-OH (24-OH-$d_6$), and ~20 pg for 25-hydroxycholesterol (25-OH), [$^2H_3$]25-OH (25-OH-$d_3$), 22R-hydroxycholesterol (22R-OH), 24S,25-epoxycholesterol (24S,25-Epoxy), and [$^2H_6$]24,25-Epoxy (24,25-Epoxy-$d_6$). The numbers on the right side of each chromatogram represent the full scale of the chromatogram.

TABLE 3. Reproducibility of the quantification of each oxysterol in rat liver microsomes

| Oxysterol | Mean ± SD (n = 12) | Relative SD | |
|---|---|---|---|
| | | Sample Preparation | Error (SRM) |
| | *ng* | % | |
| 4β-Hydroxycholesterol | 5.56 ± 0.28 | 3.3 | 5.6 |
| 7α-Hydroxycholesterol | 4.22 ± 0.13 | 3.7 | 2.9 |
| 22R-Hydroxycholesterol | 0.107 ± 0.013 | 12.7 | 11.9 |
| 24S-Hydroxycholesterol | 0.104 ± 0.007 | 8.7 | 5.8 |
| 25-Hydroxycholesterol | 0.64 ± 0.02 | 1.8 | 3.7 |
| 27-Hydroxycholesterol | 3.16 ± 0.23 | 8.1 | 6.9 |
| 24S,25-Epoxycholesterol | 1.11 ± 0.08 | 5.1 | 8.4 |

Each oxysterol was quantified in 1 mg protein from normal rat liver microsomes. Four samples were prepared and quantified in triplicate by liquid chromatography-tandem mass spectrometry. The results were analyzed by a one-way layout, in which the analytical errors were divided into two sources: sample preparation and SRM measurement.

oxysterol calculated by linear regression analysis; this also constituted an index for the precision and accuracy of the method (see supplementary Table III).

## DISCUSSION

Neutral monohydroxysterols are poorly ionized by electrospray. To overcome this disadvantage, we have developed a new method for the enhancement of the ionization efficiency by derivatizing into picolinyl esters (23, 27). Dihydroxy- or epoxysterols are more efficiently ionized by electrospray, and their limit of detection (5–60 fmol on-column) was reported to be more than 10 times lower than that of monohydroxysterols (175–2,000 fmol on-column)

TABLE 4. Recovery of each oxysterol from rat liver microsomes

| Oxysterol | Amount Added | Average Recovery[a] (Mean ± SD) (n = 6) |
|---|---|---|
| | *ng* | % |
| 4β-Hydroxycholesterol | 2.00 | 102.7 ± 8.7 |
| | 4.00 | 98.5 ± 9.9 |
| | 6.00 | 104.3 ± 11.7 |
| 7α-Hydroxycholesterol | 4.00 | 89.5 ± 7.1 |
| | 8.00 | 86.7 ± 6.9 |
| | 12.00 | 90.8 ± 8.8 |
| 22R-Hydroxycholesterol | 0.05 | 103.0 ± 15.5 |
| | 0.10 | 105.2 ± 6.9 |
| | 0.15 | 99.8 ± 5.6 |
| 24S-Hydroxycholesterol | 0.05 | 107.3 ± 14.0 |
| | 0.10 | 100.3 ± 8.4 |
| | 0.15 | 102.0 ± 9.0 |
| 25-Hydroxycholesterol | 0.20 | 106.6 ± 12.7 |
| | 0.40 | 100.1 ± 6.8 |
| | 0.60 | 103.1 ± 5.3 |
| 27-Hydroxycholesterol | 1.00 | 98.2 ± 15.0 |
| | 2.00 | 102.6 ± 4.8 |
| | 3.00 | 103.7 ± 2.2 |
| 24S,25-Epoxycholesterol | 0.40 | 97.5 ± 15.2 |
| | 0.80 | 107.2 ± 18.5 |
| | 1.20 | 104.2 ± 7.5 |

Known amounts of each oxysterol were spiked into 1 mg protein from normal rat liver microsomes before sample preparation.

[a] Recovery (%) = (amount found − *X0*)/amount added × 100. *X0* value was obtained from TABLE 3. (See Table 5 in ref. 35.)

(22). In this paper, we have studied the usefulness of our derivatization method on dihydroxy- and epoxysterols that are key regulatory oxysterols in biological samples. The detection limits of oxysterol dipicolinates and epoxycholesterol picolinate were 5–25 amol on-column, which was about 1,000-fold more sensitive than those with the underivatized ESI method (22). We also determined the detection limits of native dihydroxy- and epoxysterols by LC-APCI-MS/MS analysis, and they were about 10 fmol on-column (data not shown). Thus, highly sensitive LC-MS/MS analysis after picolinyl ester derivatization can be used not only for monohydroxysterols but also for dihydroxy- and epoxysterols.

A few derivatization methods that are suitable for LC-ESI-MS/MS analysis of dihydroxysterols have been reported. Griffiths et al. (28) converted oxysterols with a 3β-hydroxy-$\Delta^5$ structure into 3-oxo-$\Delta^4$ steroids by using cholesterol oxidase, and then derivatized with the Girard P reagent to Girard P hydrazone. This method improved the sensitivity by enhancing ionization and was successfully applied to the identification of oxysterols in the brain (29). However, this method has several disadvantages for simple and highly sensitive quantification of oxysterols in biological samples. First, two steps are needed to convert 3β-hydroxysterols into Girard P hydrazone derivatives. Second, the derivatization gives *syn* and *anti* forms with different retention times. Third, 3β-hydroxysterols with an oxo group are converted to the mono- and bis-Girard P hydrazone derivatives. Finally, this method produces the same derivative from 7α-hydroxycholesterol and 7α-hydroxy-4-cholesten-3-one, which are important intermediates in the hepatic bile acid biosynthetic pathway.

Recently, Jiang, Ory, and Han (30) reported another derivatizing method that converted oxysterols into dimethylglycine esters. This method appears to have overcome the weaknesses of the above Girard P hydrazone derivatives. However, overnight incubation at 50°C was necessary to make the dimethylglycine esters, and the formed dimethylglycine diesters provided a doubly protonated ion. MS/MS spectra of doubly protonated ions are more complicated than those of singly protonated ions. Therefore, singly charged ions are preferable as precursor ions for simple and highly sensitive MS/MS analysis.

In our picolinyl ester derivatization, Yamashita et al. (31) reported in a recent study that estradiol dipicolinates gave singly charged ions in the positive ESI mass spectrum. In the present study, oxysterols with two hydroxyl groups were also derivatized to picolinyl diesters showing singly charged ions in the positive ESI mass spectra, which appears to be a general characteristic of the picolinyl ester derivatization of steroids with two hydroxyl groups. Because of the better ionizing efficiency due to the double picolinyl moieties and a simple MS/MS spectra, the detection limits of dihydroxysterols (5–25 amol on-column) were about 100 times lower than those of monohydroxysterols (260–2,600 amol on-column) (23).

In addition, our method made it possible to quantify 24S,25-epoxycholesterol in biological samples with high sensitivity (12.5 amol on-column) and specificity. Although

this epoxycholesterol appears to be one of the most important regulatory oxysterols for cholesterol homeostasis (10, 14), the concentrations in biological samples have not been determined widely because of instability during GC-MS analysis and insufficient sensitivity by HPLC with UV detection (16). In fact, we have measured this epoxycholesterol concentration in hepatic tissues by high-resolution GC-MS after trimethylsilyl (TMS) ether derivatization (32). However, the derivative became decomposed during GC separation, giving several peaks with similar mass spectra, and 100 fmol of 24S,25-epoxycholesterol was barely detectable on-column. Although this sensitivity exceeded that obtained by the HPLC-UV method (16), it was still not sufficient to quantify this epoxycholesterol in small amounts of biological samples.

Another merit of highly sensitive quantification is that the loading amount on the HPLC column can be minimized, so that the solid-phase extraction/purification step was omitted in our assay. In human serum analysis, less than 20 pg of oxysterol picolinates was injected on the column with approximately 200 ng of cholesterol picolinate. Under our HPLC conditions, this amount of cholesterol picolinate was easily trapped in the column and eluted around 29 min, which was well separated from oxysterols and did not affect the separation or elution of each oxysterol picolinate. HPLC column separation was very important in the present method because many oxysterols have the same molecular weight and MS spectrum. By changing the collision energies, the specific MS/MS spectrum of each oxysterol was observed to some extent, but we selected less-specific SRM ion pairs rather than more-specific ones because the former showed higher sensitivities and better signal-to-noise ratios compared with the latter.

The procedure for picolinyl ester derivatization was essentially the same as that in our previous report (23), but a few modifications were made. First, the reagent mixture was prepared by using pyridine instead of tetrahydrofuran, and the incubation was performed at 80°C for 60 min. Usually, this esterification progresses easily at room temperature, but the only hydroxyl at the C-25 position of 25-hydroxycholesterol was resistant to picolinyl ester formation. However, complete esterification of this C-25 position was achieved by heating at 80°C for 60 min. After the derivatization step, excess reagents were precipitated by the addition of *n*-hexane, and picolinyl ester derivatives were recovered in the supernatant.

Serum total (free + esterified) oxysterol concentrations in 19 normal volunteers were measured by our LC-ESI-MS/MS method (**Table 5**), and the concentrations of 4β-hydroxycholesterol, 7α-hydroxycholesterol, 22R-hydroxycholesterol, 25-hydroxycholesterol, and 24S,25-epoxycholesterol looked higher than those determined by previous methods. However, 7α-hydroxycholesterol levels determined by our method did not differ significantly ($P > 0.05$) from those by the GC-MS method (33), and 22R-hydroxycholesterol and 24S,25-epoxycholesterol levels appeared to be less than the detection limits by the HPLC method (34). We cannot exclude the possibility that some 25-hydroxycholesterol was produced by cholesterol autoxidation, but it is also possible that the concentration was not quantified accurately by the low-resolution GC-MS method. This is because the TMS ether derivative of 25-hydroxycholesterol did not give an ideal mass spectrum in the high mass region and *m/z* 131 was used for the quantification by selected ion monitoring. In general, high background noise is expected when a low mass number is selected as a monitoring ion for GC-MS analysis of biological samples. We have measured 25-hydroxycholesterol and 4β-hydroxycholesterol concentrations by using different SRM ion pairs [*m/z* 635 → 146 (22 V) and *m/z* 635 → 512 (20 V), respectively], and virtually the same results have been obtained.

A recent study using Cyp27a1 knockout mice demonstrated that 25-hydroxycholesterol was also synthesized by CYP27A1 (6). Our results showed that not only 27-hydroxycholesterol but also 25-hydroxycholesterol concentrations were markedly lower in serum from a patient with CTX, CYP27A1 deficiency, compared with that from a control subject (Fig. 2C, D), which lends support to the idea that a portion of the 25-hydroxycholesterol circulating in human serum is derived from CYP27A1.

In summary, we have developed a very sensitive and specific method for the quantification of key regulatory oxysterols in biological samples. Derivatization of dihydroxy- and epoxysterols into the picolinyl esters allowed them to be quantified by LC-ESI-MS/MS with excellent sensitivity and reliability. This method is useful for the study of

TABLE 5. Concentrations of total (free + esterified) oxysterols in normal human serum: comparison with previous methods

| | Present Method | Previous Methods | |
|---|---|---|---|
| Oxysterol | Mean ± SD (n = 19) | Mean ± SD (n) | Method (Reference) |
| | *ng/ml* | *ng/ml* | |
| 4β-Hydroxycholesterol | 77 ± 40 | 29 ± 10 (125) | GC-MS (2) |
| 7α-Hydroxycholesterol | 145 ± 82 | 99 ± 43 (12) 43 ± 48 (31) | GC-MS (33) GC-MS (1) |
| 22R-Hydroxycholesterol | 10 ± 18 | ND (2) | HPLC (34) |
| 24S-Hydroxycholesterol | 51 ± 12 | 64 ± 24 (31) 64 ± 14 (22) | GC-MS (1) LC-APCI-MS (20) |
| 25-Hydroxycholesterol | 31 ± 11 | 2 ± 3 (22) | GC-MS (1) |
| 27-Hydroxycholesterol | 117 ± 35 | 154 ± 43 (31) 120 ± 30 (22) | GC-MS (1) LC-APCI-MS (20) |
| 24S,25-Epoxycholesterol | 2 ± 2 | ND (2) | HPLC (34) |

LC-APCI-MS, liquid chromatography-atmospheric pressure chemical ionization-mass spectrometry; ND, not detectable.

lipid metabolism controlled by oxysterols as well as the screening and diagnosis of metabolic disorders in oxysterols.

The authors wish to thank the late Dr. Hiroshi Miyazaki for his helpful advice regarding mass spectrometry.

## REFERENCES


1. Dzeletovic, S., O. Breuer, E. Lund, and U. Diczfalusy. 1995. Determination of cholesterol oxidation products in human plasma by isotope dilution-mass spectrometry. *Anal. Biochem.* **225:** 73–80.
2. Bodin, K., L. Bretillon, Y. Aden, L. Bertilsson, U. Broome, C. Einarsson, and U. Diczfalusy. 2001. Antiepileptic drugs increase plasma levels of 4β-hydroxycholesterol in humans: evidence for involvement of cytochrome p450 3A4. *J. Biol. Chem.* **276:** 38685–38689.
3. Pikuleva, I. A. 2006. Cholesterol-metabolizing cytochromes P450. *Drug Metab. Dispos.* **34:** 513–520.
4. Lund, E. G., T. A. Kerr, J. Sakai, W. P. Li, and D. W. Russell. 1998. cDNA cloning of mouse and human cholesterol 25-hydroxylases, polytopic membrane proteins that synthesize a potent oxysterol regulator of lipid metabolism. *J. Biol. Chem.* **273:** 34316–34327.
5. Lund, E. G., J. M. Guileyardo, and D. W. Russell. 1999. cDNA cloning of cholesterol 24-hydroxylase, a mediator of cholesterol homeostasis in the brain. *Proc. Natl. Acad. Sci. USA.* **96:** 7238–7243.
6. Li, X., W. M. Pandak, S. K. Erickson, Y. Ma, L. Yin, P. Hylemon, and S. Ren. 2007. Biosynthesis of the regulatory oxysterol, 5-cholesten-3β,25-diol 3-sulfate, in hepatocytes. *J. Lipid Res.* **48:** 2587–2596.
7. Smith, L. L. 1981. Cholesterol Autoxidation. Plenum Press, New York.
8. Nelson, J. A., S. R. Steckbeck, and T. A. Spencer. 1981. Biosynthesis of 24,25-epoxycholesterol from squalene 2,3;22,23-dioxide. *J. Biol. Chem.* **256:** 1067–1068.
9. Janowski, B. A., P. J. Willy, T. R. Devi, J. R. Falck, and D. J. Mangelsdorf. 1996. An oxysterol signalling pathway mediated by the nuclear receptor LXRα. *Nature.* **383:** 728–731.
10. Janowski, B. A., M. J. Grogan, S. A. Jones, G. B. Wisely, S. A. Kliewer, E. J. Corey, and D. J. Mangelsdorf. 1999. Structural requirements of ligands for the oxysterol liver X receptors LXRα and LXRβ. *Proc. Natl. Acad. Sci. USA.* **96:** 266–271.
11. Fu, X., J. G. Menke, Y. Chen, G. Zhou, K. L. MacNaul, S. D. Wright, C. P. Sparrow, and E. G. Lund. 2001. 27-Hydroxycholesterol is an endogenous ligand for liver X receptor in cholesterol-loaded cells. *J. Biol. Chem.* **276:** 38378–38387.
12. Axelson, M., and O. Larsson. 1995. Low density lipoprotein (LDL) cholesterol is converted to 27-hydroxycholesterol in human fibroblasts. *J. Biol. Chem.* **270:** 15102–15110.
13. Krieger, M., J. L. Goldstein, and M. S. Brown. 1978. Receptor-mediated uptake of low density lipoprotein reconstituted with 25-hydroxycholesteryl oleate suppresses 3-hydroxy-3-methylglutaryl-coenzyme A reductase and inhibits growth of human fibroblasts. *Proc. Natl. Acad. Sci. USA.* **75:** 5052–5056.
14. Spencer, T. A., A. K. Gayen, S. Phirwa, J. A. Nelson, F. R. Taylor, A. A. Kandutsch, and S. K. Erickson. 1985. 24(S),25-Epoxycholesterol. Evidence consistent with a role in the regulation of hepatic cholesterogenesis. *J. Biol. Chem.* **260:** 13391–13394.
15. Breuer, O., and I. Björkhem. 1990. Simultaneous quantification of several cholesterol autoxidation and monohydroxylation products by isotope-dilution mass spectrometry. *Steroids.* **55:** 185–192.
16. Zhang, Z., D. Li, D. E. Blanchard, S. R. Lear, S. K. Erickson, and T. A. Spencer. 2001. Key regulatory oxysterols in liver: analysis as $\Delta^4$-3-ketone derivatives by HPLC and response to physiological perturbations. *J. Lipid Res.* **42:** 649–658.
17. Ogishima, T., and K. Okuda. 1986. An improved method for assay of cholesterol 7α-hydroxylase activity. *Anal. Biochem.* **158:** 228–232.
18. Hylemon, P. B., E. J. Studer, W. M. Pandak, D. M. Heuman, Z. R. Vlahcevic, and Y. L. Chiang. 1989. Simultaneous measurement of cholesterol 7α-hydroxylase activity by reverse-phase high-performance liquid chromatography using both endogenous and exogenous [4-$^{14}$C]cholesterol as substrate. *Anal. Biochem.* **182:** 212–216.
19. Teng, J. I., and L. L. Smith. 1995. High-performance liquid chromatographic analysis of human erythrocyte oxysterols as $\Delta^4$-3-ketone derivatives. *J. Chromatogr. A.* **691:** 247–254.
20. Burkard, I., K. M. Rentsch, and A. von Eckardstein. 2004. Determination of 24S- and 27-hydroxycholesterol in plasma by high-performance liquid chromatography-mass spectrometry. *J. Lipid Res.* **45:** 776–781.
21. Saldanha, T., A. C. Sawaya, M. N. Eberlin, and N. Bragagnolo. 2006. HPLC separation and determination of 12 cholesterol oxidation products in fish: comparative study of RI, UV, and APCI-MS detectors. *J. Agric. Food Chem.* **54:** 4107–4113.
22. McDonald, J. G., B. M. Thompson, E. C. McCrum, and D. W. Russell. 2007. Extraction and analysis of sterols in biological matrices by high performance liquid chromatography electrospray ionization mass spectrometry. *Methods Enzymol.* **432:** 145–170.
23. Honda, A., K. Yamashita, H. Miyazaki, M. Shirai, T. Ikegami, G. Xu, M. Numazawa, T. Hara, and Y. Matsuzaki. 2008. Highly sensitive analysis of sterol profiles in human serum by LC-ESI-MS/MS. *J. Lipid Res.* **49:** 2063–2073.
24. Honda, A., G. Salen, Y. Matsuzaki, A. K. Batta, G. Xu, E. Leitersdorf, G. S. Tint, S. K. Erickson, N. Tanaka, and S. Shefer. 2001. Differences in hepatic levels of intermediates in bile acid biosynthesis between Cyp27−/− mice and CTX. *J. Lipid Res.* **42:** 291–300.
25. Honda, A., Y. Mizokami, Y. Matsuzaki, T. Ikegami, M. Doy, and H. Miyazaki. 2007. Highly sensitive assay of HMG-CoA reductase activity by LC-ESI-MS/MS. *J. Lipid Res.* **48:** 1212–1220.
26. Taguchi, G. 1986. Introduction to Quality Engineering-Designing Quality into Products and Process. Asian Productivity Organization, Tokyo, Japan.
27. Yamashita, K., S. Kobayashi, S. Tsukamoto, and M. Numazawa. 2007. Synthesis of pyridine-carboxylate derivatives of hydroxysteroids for liquid chromatography-electrospray ionization-mass spectrometry. *Steroids.* **72:** 50–59.
28. Griffiths, W. J., Y. Wang, G. Alvelius, S. Liu, K. Bodin, and J. Sjövall. 2006. Analysis of oxysterols by electrospray tandem mass spectrometry. *J. Am. Soc. Mass Spectrom.* **17:** 341–362.
29. Karu, K., M. Hornshaw, G. Woffendin, K. Bodin, M. Hamberg, G. Alvelius, J. Sjövall, J. Turton, Y. Wang, and W. J. Griffiths. 2007. Liquid chromatography-mass spectrometry utilizing multi-stage fragmentation for the identification of oxysterols. *J. Lipid Res.* **48:** 976–987.
30. Jiang, X., D. S. Ory, and X. Han. 2007. Characterization of oxysterols by electrospray ionization tandem mass spectrometry after one-step derivatization with dimethylglycine. *Rapid Commun. Mass Spectrom.* **21:** 141–152.
31. Yamashita, K., M. Okuyama, Y. Watanabe, S. Honma, S. Kobayashi, and M. Numazawa. 2007. Highly sensitive determination of estrone and estradiol in human serum by liquid chromatography-electrospray ionization tandem mass spectrometry. *Steroids.* **72:** 819–827.
32. Honda, A., G. Salen, Y. Matsuzaki, A. K. Batta, G. Xu, T. Hirayama, G. S. Tint, M. Doy, and S. Shefer. 2005. Disrupted coordinate regulation of farnesoid X receptor target genes in a patient with cerebrotendinous xanthomatosis. *J. Lipid Res.* **46:** 287–296.
33. Oda, H., H. Yamashita, K. Kosahara, S. Kuroki, and F. Nakayama. 1990. Esterified and total 7α-hydroxycholesterol in human serum as an indicator for hepatic bile acid synthesis. *J. Lipid Res.* **31:** 2209–2218.
34. Kudo, K., G. T. Emmons, E. W. Casserly, D. P. Via, L. C. Smith, J. St Pyrek, and G. J. Schroepfer, Jr. 1989. Inhibitors of sterol synthesis. Chromatography of acetate derivatives of oxygenated sterols. *J. Lipid Res.* **30:** 1097–1111.
35. Honda, A., K. Yamashita, H. Miyazaki, M. Shirai, T. Ikegami, G. Xu, M. Numazawa, T. Hara, and Y. Matsuzaki. 2008. Highly sensitive analysis of sterol profiles in human serum by LC-ESI-MS/MS. *J. Lipid Res.* **49:** 2063–2073.

*Hepatology Research* 2009; 39: 341–345 doi: 10.1111/j.1872-034X.2008.00460.x

*Original Article*

# Impact of determination of hepatitis B virus subgenotype and pre-core/core-promoter mutation for the prediction of acute exacerbation of asymptomatic carriers

Tadashi Ikegami,[1,2] Yasuhiko Matsuki,[2] Yasuhito Tanaka,[3] Masashi Mizokami,[3] Akira Honda,[4] Takeshi Hirayama,[1] Yoshifumi Saito[1] and Yasushi Matsuzaki[1]

[1]*Division of Gastroenterology and Hepatology, and* [4]*Collaborative Research Center, Tokyo Medical University, Kasumigaura Hospital, Inashiki-gun, and* [2]*Department of Medicine, Tsukuba Gakuen Hospital, Tsukuba City, and* [3]*Department of Clinical Molecular Informative Medicine, Nagoya City University Graduate School of Medical Sciences, Nagoya, Japan*

*Aim:* A large cohort study in Japan revealed that the specific viral profile may influence the fulminant outcome in acute hepatitis B virus (HBV) infections, while the genetic influence on outcome has not been clarified in patients with acute exacerbation of chronic liver disease caused by HBV. We experienced a case of fatal liver failure that developed as the result of chronic HBV infection. To determine possible genetic factor involving acute exacerbation, genetic analysis of serum from the patient and his siblings was performed.

*Methods:* HBV subgenotype as well as pre-core/core-promoter mutations of samples mentioned above were determined.

*Results:* Patient had HBV-Bj with pre-core (1896/1899) and core-promoter (1762/1764) mutations, the genomic profile frequently seen in fulminant hepatitis caused by acute HBV infection.

*Conclusion:* This result suggests that determination of the HBV subgenotype and pre-core/core promoter mutations could provide a rationale for development of a treatment strategy in asymptomatic HBV carriers.

**Key words:** hepatits B virus (HBV), fulminant hepatitis, chronic hepatitis, subgenotype, pre-core/core promoter mutations

## INTRODUCTION

A RECENT REPORT has suggested that genotype and pre-core mutations may influence the fulminant outcome of acute hepatitis B virus (HBV) infection.[1] The report suggests that fulminant hepatitis was frequently associated with a Bj subgenotype and a lack of HBeAg, as well as high replication due to a pre-core mutation (PC) in patients with acute HBV infection. Further, 12 of 22 patients (55%) infected with HBV-Bj developed fulminant hepatitis, whereas no patients infected with HBV-Ae did, and that both PC (G1896A) and core-promoter (CP; A1762T/G1764A) mutations were significantly more frequent in patients with fulminant hepatitis compared to those with acute self-limiting hepatitis.[1]

*Correspondence: Dr Yasushi Matsuzaki, Division of Gastroenterology and Hepatology, Tokyo Medical University, Kasumigaura Hospital, 3-20-1 Chuo, Ami-machi, Inashiki-gun, Ibaraki, 300-0395, Japan. Email: ymatsuzaki-gi@umin.ac.jp*
*Received 1 August 2008; revised 29 August 2008; accepted 16 September 2008.*

The genetic influence on outcome has not been clarified in patients with acute exacerbation of chronic liver disease caused by HBV. We experienced a case of fatal liver failure that developed from chronic infection of HBV. To determine possible genetic factor involving acute exacerbation, we performed genetic analysis of serum from the patient and his siblings and obtained interesting findings. Although accumulation of data among a large number of asymptomatic carriers are needed, it is worthwhile to mention the determination of subgenotype and PC or CP mutations in asymptomatic HBV carriers may give us a rationale to predict future exacerbation of hepatitis and in turn, provide a better outcome for these patients.

## CLINICAL CASE

THE PATIENT WAS a 41-year-old man, born in Okinawa prefecture. He initially presented with general fatigue, and a physical examination and blood tests showed liver dysfunction and jaundice. He did not have any history of hospitalization. No abnormal

Table 1 Laboratory data on admission

| |
|---|
| Blood Cell Count: WBC 5850 (Stab 4.0, Seg 78.0, Lym 11.0, Mono 7.0), RBC 429 ¥ $10^4$, Hb 14.4 g/dL, Plt 11.0 ¥ $10^4$ |
| Coagulation Tests: PT 9.8% (INR 6.88), Fibrinogen 87 mg/dL, FDP 9.3 mg/mL |
| Biochemistry: Na/K/Cl 133/3.8/99 mM, TP 5.7 g/dL, Alb 3.2 g/dL |
| BUN 7.5 mg/dL, s-Cre 0.6 mg/dL |
| AST 910 U/l, ALT 1752 U/l, LDH 511 U/l, |
| ALP 708 U/l, -GTP 150 U/L, ChE 170 U/L |
| T-Bil 18.1 mg/dL, D-Bil 7.7 mg/dL (D/T = 0.425) |
| CRP 0.7 mg/dL, $NH_3$ 212 mg/dL |
| Viral Markers: HBsAg (+) (EIA titer 184.83) |
| IgM-HBc Ab (-), HBc Ab/CLIA (+) |
| HBeAg (-), HBeAb (+) (99.8% inhibition) |
| HBV-DNA/TMA 6.6 LGE/mL, HDV-DNA (-) |
| HCV-Ab (-), IgM-HA-Ab (-), HEV-DNA (-) |
| CMV-Ab IgG 10>, CMV-IgM 10> |
| EBV-anti VCA IgG ¥ 80?IgM 10> |
| Others: ANA 20.2, anti DNA antibody 80, |
| Anti Mitochondria Ab 20> |

findings were noted at annual physical check-up. He was considered to be an asymptomatic HBV carrier. The patient was hospitalized on the day of his first visit. Follow-up tests showed worsening of liver enzyme levels and an alteration in consciousness level was noticed after 2 days. The patient was then referred to Tsukuba Gakuen Hospital as the development of acute liver failure was of concern.

Laboratory data on arrival are shown in Table 1. Elevation of serum ALT (1754 IU/L) and hyperbilirubinemia (T-Bil, 18.1 mg/dL) were observed. The patient was positive for HBVs antigen and HBe antibody, but markers for other types of viral hepatitis, including hepatitis A virus, hepatitis C virus, hepatitis D virus and hepatitis E virus were all negative. The HBV-DNA level was found to be more than 6.6 log genome equivalents (LGE)/mL using transcription-mediated amplification. Prothrombin time was markedly prolonged (PT% = 20) and an atrophic liver was apparent on abdominal ultrasonography. The patient showed disorientation and pronounced confusion on the day of arrival, and thus was diagnosed with grade III hepatic encephalopathy. He was immediately placed on artificial liver support (ALS) comprising plasma exchange and hemodiafiltration[2] with a combination of interferon beta and lamivudine, only nucleic acid analog approved by Japanese National health Insurance system at this time, as antiviral therapy (Fig. 1). A large dose of methylpredonisolone was also administered to suppress a presumably enhanced host immune response.[3]

In parallel, we started to discuss liver transplantation with his family. The patient had four brothers, and three were considered as possible donors for orthopedic liver transplantation. However, screening by blood tests and ultrasonography showed that the three brothers were positive for HBs antigen, and therefore all were excluded as donor candidates. A cadaveric liver was unavailable and thus we had to give up on liver transplantation. Despite intensive care, the patient complicated with acute respiratory distress syndrome (ARDS) and acute renal failure, and died on the 8th day of admission.

## GENETIC ANALYSIS OF HBV

WITH THE PERMISSION of the family members, genetic analysis of HBV in serum acquired from the patient and family members was performed. HBV DNA sequences spanning the S gene were determined by real-time PCR according to the method of Abe *et al.*,[4] with a detection limit of 100 copies/mL. HBV DNA sequences bearing the CP, PC region, and core gene were amplified by PCR using hemi-nested primers, as described previously.[4] The neighbor-joining method[5] was used for phylogenetic analysis of the S region to classify HBV into subgenotypes. To confirm the reliability of the phylogenetic tree, bootstrap re-sampling tests were performed 1000 times.

Only the third sibling ("sibling C" in Table 2) showed an elevated ALT level (50 IU/L), with ALT levels in the

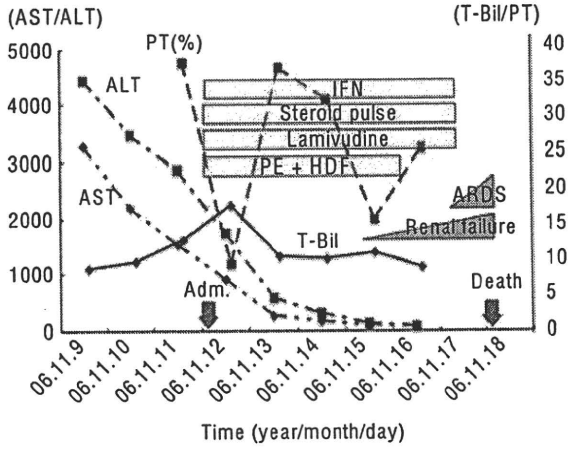


Figure 1 Clinical Course of the patient. ARDS, acute respiratory distress syndrome; HDF, hemodiafiltration; IFN, interferon beta; PE, plasma exchange; PT, prothrombin time.

Table 2 Profile of each sibling

| | Age | Sex | AST/ALT | HBV-DNA | HBeAg | 1896A/1899A/CP |
|---|---|---|---|---|---|---|
| Patient | 41 | M | 910/1752 | 6.02 log copy/mL | – | +/+/+ |
| Sibling A | 45 | M | 36/35 | 5.25 log copy/mL | – | +/–/– |
| Sibling B | 36 | M | 28/32 | 4.68 log copy/mL | – | +/–/– |
| Sibling C | 31 | M | 31/50 | <2.6 log copy/mL | – | +/+/– |

other siblings within the normal range (about 40 IU/L). None of the siblings were HBeAg-positive. HBV-DNA loads were highest in the patient, relatively lower in sibling A and B, and under the detectable range in sibling C (Table 2). The HBV genotype was determined based on analysis of the S region. All siblings were infected with HBV-Bj, a subgenotype that is predominantly detected in patients who reside in a specific geographical location (including Okinawa prefecture) in Japan. HBV-DNA of patient and all siblings formed same cluster, thus it is speculated that they were infected from same source. In fact, the presence of family history of hepatic disease (their mother died by it) strongly suggests the vertical infection (Fig. 2). Mutations in the PC (G1896A) and CP (A1762T/G1764A) were also discovered. As shown in Figure 3, the patient and all siblings had the 1896A mutation, which is consistent with the absence of HBeAg, and the patient had both the G1899A and CP mutations (A1762T/G1764A). Sibling C had the G1899A mutation but not the CP mutation, and the other siblings had none of these mutations.

## DISCUSSION

FULMINANT VIRAL HEPATITIS is thought to occur as a result of immunoreactions against enhanced viral replication. Findings associated with immunoresponses of hosts in fulminant cases are limited, probably due to the absence of definitive methodology for determination of individual immunoresponses. However, factors associated with viral replication have been investigated, and an HBV subgenotype and PC and CP mutations have been linked to high replication rates in acute HBV infection and in turn to fulminant outcome.[1] Besides fulminant hepatitis caused by acute infection of HBV, fatal acute liver failure may also emerge from a previously unrecognized chronic infection of HBV, but little is known about the viral factors involved in acute exacerbation in chronic HBV carriers.

In the current case, the patient was infected with the HBV/Bj subgenotype, was HBeAb-positive, and had PC and CP mutations. Although the patient was already an HBV carrier at the time of onset, his genomic profiles matched the pattern frequently seen in fulminant hepatitis caused by acute HBV infection.[1] Among the population of HBV carriers, patients infected with HBV/Ce and HBV/Bj are predominant in Japan.[6–9] HBV/Bj is a specific subgenotype that is present in less than 10% of HBV carriers, but has a higher prevalence in locations such as the Northeastern (Tohoku) district of Honshu and in Okinawa. Patients with HBV/C infection tend to have chronic sustained inflammation that progresses to liver cirrhosis and hepatocellular carcinoma, whereas HBV/Bj more frequently induces HBe seroconversion via a PC mutation, which results in a lower viral load and reduced disease severity.[10]

Sugiyama *et al.* determined the intracellular and extracellular HBV DNA levels in Huh-7 cells transfected with a plasmid carrying different genotypes/subgenotypes of the HBV genome without a CP/PC mutation.[11] HBV DNA levels in cell lysates were highest for HBV/C, followed by Bj/Ba and D/Ae, and lowest for Aa; whereas in culture media these levels were highest for Bj, with much lower levels for Ba/C/D, and still lower levels for Ae/Aa.[11] It was speculated that the strong tendency of Bj for extracellular virion secretion may endow a high infectious capacity to blood from individuals infected with this subgenotype, and that this may trigger strong immune responses in hosts.[11] This characteristic of HBV/Bj is thought to be associated with earlier seroconversion from hepatitis Be antigen (HBeAg) to the corresponding antibody (anti-HBe) and with lower histological activity.

Acute exacerbation of chronic liver disease (CLD) has been seen in some patients with chronic HBV/Bj infection post-seroconversion, with a fatal outcome similar to that in the current case. In a study of 592 patients, no significant difference in the frequency of genotype B was found between patients with CLD and those with acute exacerbation of CLD (62/531 [11.7%] versus 4/19 [21.1%]; NS),[12] but acute exacerbation was seen more frequently in CLD patients with HBV/B infection (4/62, 6.5%) compared to those with HBV/C infection (13/459, 2.8%).[12] The PC stop codon mutation (G1896A)

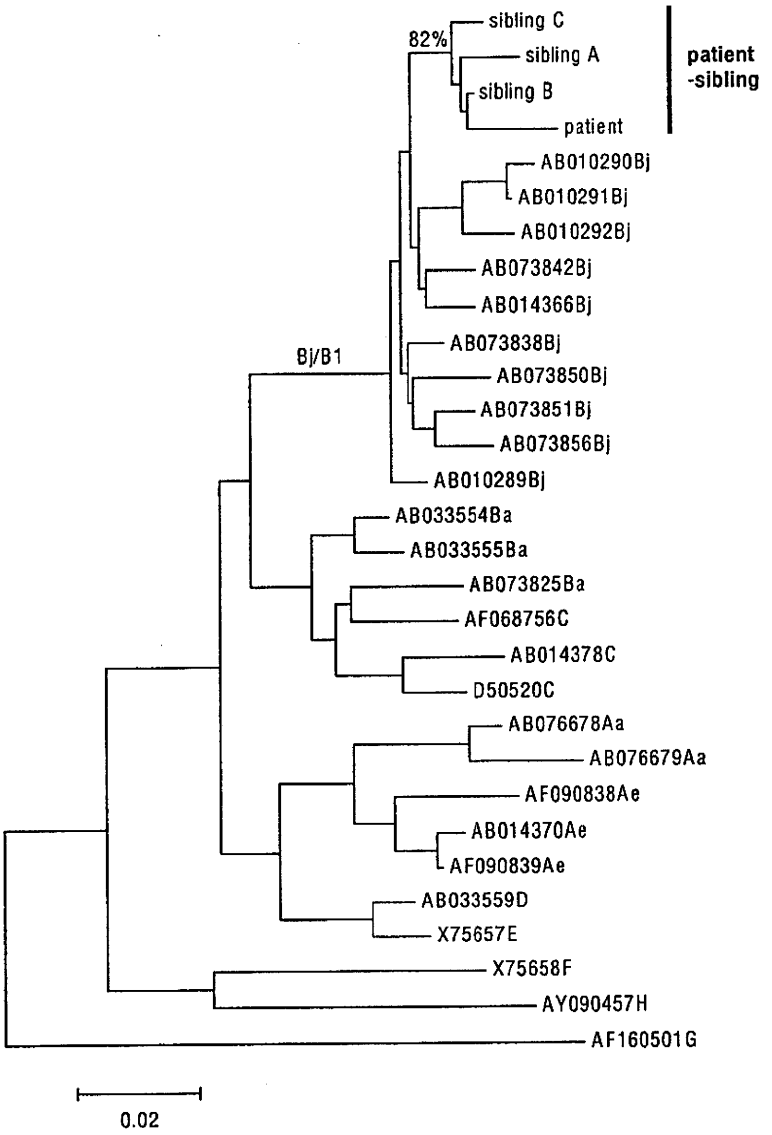


Figure 2 Subgenotyping of hepatitis B virus (HBV). HBV subgenotype was determined by sequencing of the S gene. Result of phylogenetic analysis of sequences from the pre-S region of HBV in the patient and siblings and reference strains from a database was shown. Reference strains were shown by accession number. The scale bar indicates genetic distance.

and the CP double mutation (A1762T/G1764A) were detected more frequently in HBV/Bj-infected patients with fulminant hepatitis compared to those with acute-self limited hepatitis (56% vs. 0%, and 67% vs. 0%).[1] These findings suggest that the replication potential of HBV/Bj might be stronger in the presence of CP/PC mutations than in the wild type virus, and Ozasa *et al.* demonstrated enhanced replication capacity of HBV/Bj with PC or CP mutations compared to wild type *in vitro*.[1]

Although HBV/Bj may show highly potent replication, this may not be the cause of enhanced immunoresponsiveness in patients with chronic infection of HBV/Bj. Rather, CP/PC mutation in HBV/Bj post-seroconversion may be the factor that facilitates potent viral replication and acute exacerbation of CLD. The host-associated factor that influences outcome in patients with chronic HBV/Bj infection has not been identified, but these viral characteristics may be predictive factors for future exacerbation. In the current study, the patient had both PC (G1896A/G1899A) and CP mutations and a G1896A/G1899A mutation was found in one sibling. Although HBV-DNA load in this sibling is under detectable range right now, a CP mutation in the future on this sibling may lead to a fatal outcome.

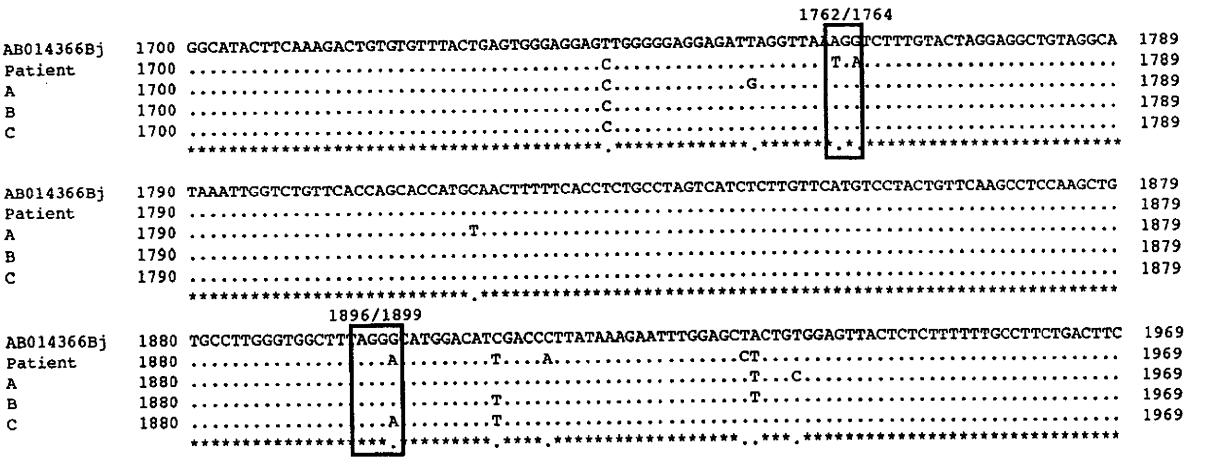


Figure 3 Nucleotide sequence of the core promoter/pre core region. Core promoter and pre-core region of hepatitis B virus (HBV) in the patient and siblings were determined. Mutation in core promoter (A1762T, G1764A) and precore (G1896A, G1899A) are indicated in boxes. The sequence of the reference HBV/Bj (AB014366Bj) is shown at the top of the figure.

Therefore, this sibling requires intensive follow-up and possible early administration of anti-viral drugs especially under the condition with immunosuppression, which can facilitate viral replication.

In conclusion, we suggest that analysis of the HBV subgenotype and CP/PC mutations should be performed during observation of asymptomatic HBV carriers to provide a more accurate understanding of the clinical presentation and to build an appropriate treatment strategy.

## REFERENCES

1 Ozasa A, Tanaka Y, Orito E *et al.* Influence of genotypes and precore mutations on fulminant or chronic outcome of acute hepatitis B virus infection. *Hepatology* 2006; 44: 326–34.

2 Yoshiba M, Inoue K, Sekiyama K, Koh I. Favorable effect of new artificial liver support on survival of patients with fulminant hepatic failure. *Artif Organs* 1996; 20: 1169–72.

3 Masuhara M, Yagawa T, Aoyagi M *et al.* HBV-related fulminant hepatic failure: successful intensive medical therapy in a candidate for liver transplantation. *J Gastroenterol* 2001; 36: 350–3.

4 Abe A, Inoue K, Tanaka T *et al.* Quantitation of hepatitis B virus genomic DNA by real-time detection PCR. *J Clin Microbiol* 1999; 37: 2899–903.

5 Saitou N, Nei M. The neighbor-joining method: a new method for reconstructing phylogenetic trees. *Mol Biol Evol* 1987; 4: 406–25.

6 Sugauchi F, Orito E, Ichida T *et al.* Epidemiologic and virologic characteristics of hepatitis B virus genotype B having the recombination with genotype C. *Gastroenterology* 2003; 124: 925–32.

7 Tanaka Y, Orito E, Yuen MF *et al.* Two subtypes (subgenotypes) of hepatitis B virus genotype C: a novel subtyping assay based on restriction fragment length polymorphism. *Hepatol Res* 2005; 33: 216–24.

8 Takeda Y, Katano Y, Hayashi K *et al.* Difference of HBV genotype distribution between acute hepatitis and chronic hepatitis in Japan. *Infection* 2006; 34: 201–7.

9 Hayashi K, Katano Y, Takeda Y *et al.* Comparison of hepatitis B virus subgenotypes in patients with acute and chronic hepatitis B and absence of lamivudine-resistant strains in acute hepatitis B in Japan. *J Med Virol* 2007; 79: 366–73.

10 Hagiwara S, Kudo M, Minami Y *et al.* Clinical significance of the genotype and core promoter/pre-core mutations in hepatitis B virus carriers. *Intervirology* 2006; 49: 200–6.

11 Sugiyama M, Tanaka Y, Kato T *et al.* Influence of hepatitis B virus genotypes on the intra- and extracellular expression of viral DNA and antigens. *Hepatology* 2006; 44: 915–24.

12 Imamura T, Yokosuka O, Kurihara T *et al.* Distribution of hepatitis B viral genotypes and mutations in the core promoter and precore regions in acute forms of liver disease in patients from Chiba, Japan. *Gut* 2003; 52: 1630–7.

*Hepatology Research* 2009; 39: 585–594 doi: 10.1111/j.1872-034X.2009.00495.x

***Original Article***

# Regulatory T cells and liver pathology in a murine graft versus host response model

Teruo Miyazaki,[1,2] Mikio Doy,[3] Tadashi Ikegami,[4] Akira Honda,[1,2] Rie Unno,[5] Shinichi Itoh,[4] Bernard Bouscarel[6] and Yasushi Matsuzaki[1,4]

*[1]Department of Development for Community Medicine, Tokyo Medical University, [2]Center for Collaborative Research, Tokyo Medical University Ibaraki Medical Center, [4]Department of Internal Medicine, Division of Gastroenterology and Hepatology, Tokyo Medical University Ibaraki Medical Center, Ami, [3]Ibaraki Prefectural Central Hospital, Kasama, [5]Unno Clinic, Moriya, Japan; and [6]Department of Biochemistry and Molecular Biology, The George Washington University, District of Columbia, USA*

*Aim:* We have previously reported in mice the hepatic inflammatory in graft versus host response (GVHR) model due to the disparity of major histocompatibility complex class-II. The regulatory T (Treg) cells have been reported to control excessive immune response and prevent immune-related diseases. This study aimed to investigate the pathogenesis profiles of chronic GVHR progression, focusing on the Treg cells.

*Methods:* GVHR mice induced by parental spleen $CD4^+$ T cell injection were sacrificed after 0, 2, 4, and 8 weeks (G0, G2, G4, G8). Further, one GVHR group received anti-IL-10 antibody in advance and were maintained for 2 weeks. Pathologic profiles of hepatic infiltrating inflammatory cells were evaluated by haematoxylin and eosin and immunohistochemistry staining with surface markers including Treg cell markers.

*Results:* Remarkable hepatic inflammatory in G2 significantly and gradually improved over time up to G8. In immunohistochemical staining, the increased IL-10 receptor $\beta^+$ Tr1 cells in G2 were maintained through to G8; although other inflammatory cells decreased from G2 to G8. By contrast, in the anti-IL-10 antibody received-GVHR mice, the Tr1 cells were not detectable with significant inflammatory aggravation, while $FoxP3^+$ Treg cells significantly enhanced.

*Conclusions:* These findings in the GVHR mice suggest that the expression and activity of Treg cells, especially the Tr1 cells, might be key factors for pathologic alteration in immune-related liver disease.

**Key words:** Graft versus host response disease, Immunohistochemistry staining, Regulatory T cells, Tr1 cells

## INTRODUCTION

WE HAVE PREVIOUSLY reported that the injection of parental $CD4^+$ T cells into F1 hybrid mice induced graft versus host response (GVHR) hepatitis due to the disparity of the major histocompatibility complex (MHC) class II.[1-5] The GVHR mice have histological and immunological alterations similar to those observed in primary biliary cirrhosis (i.e. infiltration of lymphocytes in the periportal region, pericholangitis around the interlobular bile duct, and the presence of anti-mitochondrial antibodies of a recipient origin).[6] In the histological and immunological observations of the GVHR model over a period of 2 weeks, the inflammatory cells, including $CD4^+$T cells, $CD8^+$T cells, B cells, and macrophages, infiltrated into the hepatic tissue as early as 3 days after the parental T cell transfer, and the inflammation developed within 2 weeks. Differential profiles of inflammatory-related cytokines were observed in the hepatic tissues between Th1- and Th2-derived cytokines in a manner that was dependent on the GVHR progression during this period.[2] A significantly higher level of interferon (IFN)-γ mRNA was observed after 3 days and was maintained for at least 2 weeks. On the other hand, the interleukin (IL)-10 mRNA expression was not detectable at 3 days, but was significantly increased by the 2-week time point.

Notably, the GVHR model does not lead to liver cirrhosis, because the serum aminotransferases levels

*Correspondence: Dr Yasushi Matsuzaki, Department of Internal Medicine, Division of Gastroenterology and Hepatology, Tokyo Medical University Ibaraki Medical Center, 3-20-1, Chuo, Ami, Ibaraki, Japan. 300-0395. Email: ymatsuzaki-gi@umin.ac.jp*
*Received 15 October 2008; revision 12 November 2008; accepted 26 December 2008.*

remained unchanged throughout the study period and fibrosis did not appear after 2 weeks.[2–5] It has been considered that the GVHR would cause abrogation of immune-tolerance because the transferred parental T cells invade at the site of the hepatic lesions due to the differences in MHC class II.[7] The abrogation of self-tolerance has been known to cause autoimmune diseases,[8] and can be prevented by the regulatory T (Treg) cells, which are a subset of the $CD4^+$T cells.[9–11] The Treg cells play important roles in controlling excessive immune response and preventing immune-related diseases.[10] The Treg cells can be characterized into different subsets based on surface markers, cytokine profiles, and suppressing functions; $CD4^+CD25^+$Treg cells, IL-10 receptor $(R)^+$ type 1 Treg (Tr1) cells, and $CD4^+CD161^+$ natural killer T (NKT) cells.[10,12,13]

We hypothesized that the Treg cells might influence the progression of the liver pathology in the GVHR, because this model shows abrogation of immune-tolerance. In the present study, we investigated the pathogenesis profiles on the progression of chronic GVHR over a period of 8 weeks, focusing on the time-dependent relationship between the progression of the inflammatory lesions and the expression of the Treg cells in the hepatic tissue by histological analyses.

## MATERIALS AND METHODS

### GVHR animal model

C57BL/6(B6)[*H-2K*$^b$, *I-A*$^b$, *H-2D*$^b$] mice were purchased from the Charles River Japan (Atsugi, Japan). B6.*C-H-2*$^{bm/2}$(bm12)[*H-2K*$^b$, *I-A*$^{bm12}$, *H-2D*$^b$] mice with mutation at the I-A region, originally from the Jackson Laboratory (Bar Harbor, ME, USA), were used to obtain (bm12 × B6) F1 hybrid mice. All animals received humane care in accordance with the guidelines of the University of Tsukuba for the care of laboratory animals.

Female F1 mice, between 10 and 15 weeks of age, received donor B6 T cells for the induction of GVHR as previously reported.[5,14] Briefly, sex-matched $1–2 \times 10^7$ B6 T cells were injected into recipients via the tail vein. Five recipient mice were sacrificed immediately, or 2, 4, and 8 weeks after the cell transfer (G0, G2, G4, G8). Furthermore, the anti-IL-10 monoclonal antibody (mAb)-injected GVHR model mice were induced according the method described in our previous study.[5] Either the IL-10 mAb (JESO52A55 Genzyme/Techne, Cambridge, MA, USA) or control mAb (Rat IgG1 Isotype Control, 43414.11 Genzyme/Techne) dissolved in pathogen-free saline were injected intraperitoneally at a dose of 500 mg per mouse 4 h before the cell transfer, and five mice per group were sacrificed at 2 weeks. Anaesthetized with pentobarbital, the liver was perfused with 2 mL PBS via the portal vein to washout the blood from the liver. Tissues including liver, spleen, lung, heart, kidneys, and bone marrow were embedded in paraffin after fixation in 10% formalin for histological studies including including Haematoxylin and eosin (H&E) and immunohistochemical (IHC) stains.

### H&E stain

The H&E staining was conducted using a standard method. The H&E images were captured into a computer, and the areas of infiltration of inflammatory cells into the hepatic tissue were analyzed using Image J software (NIH, Bethesda, MA, USA). In addition, the numbers of total inflammatory cells in the lesion were counted.

### IHC stain

IHC stain was carried out using the auto-stain Discovery-XT system with the proprietary reagents (Ventana, Tucson, AZ, USA). In the case of mouse monoclonal antibodies, the MoMap kit (Ventana) was used to avoid any reactions with non-specific antigens in mouse tissues. The mouse antibody was previously reacted with biotin-conjugated anti-mouse IgG antibody, and then, applied to the tissue slide after deactivation of any non-reacted IgG antibodies by reaction with mouse serum. The monoclonal antibodies used were as follows: CD4; CD8; CD20 (pre-diluted; Ventana), CD45ro (1:100; Chemicon International, Temecula, CA, USA), CD25; IL-2Rα (surface marker for $CD4^+CD25^+$Treg cells; pre-diluted; Lab vision, Fremont, CA, USA), X-linked forkhead/winged helix transcription factor (Foxp3; master gene of $CD4^+CD25^+$Treg cells; 1:100; Affinity Bioreagent, Golden, CO, USA).[12,15–18] The polyclonal antibodies were as follows; CD161 (1:100; Santa Cruz, CA, USA), IL-10Rβ (surface marker for the Tr1 cells; 1:100; Sigma, St. Louis, MO, USA). The slides were incubated with the primary antibody for one hour at 37 °C, and then, incubated with the biotin-conjugated universal secondary antibody (Ventana) for 32 min at 37 °C. The development was performed using the DAB map kit (Ventana), and nucleus and cytoplasm were stained using the hematoxylin counterstain (Ventana) and bluing reagent (Ventana).

In the IHC stain, the positive cells to the respective antibody were counted, and the ratio of the positive cells in the G2, G4, and G8 to total inflammatory cells in G2 were calculated.

### Fluorescence double IHC stain

The CD25&CD4, IL-10Rβ&CD4, or CD161&CD4 double positive cells of the infiltrated inflammatory cells at G2 were examined by fluorescence IHC double stain and detected by a laser confocal microscopy (FV1000, Olympus, Tokyo, Japan). In the CD25&CD4 double stain, the CD4 antibody and FITC-conjugated anti-mouse antibody (1:500, Santa Cruz), and the CD25 antibody and Texas Red (TR)-conjugated anti-mouse IgG antibody (1:500, Santa Cruz) were reacted in a tube in advance using the MoMap kit, respectively, and then, the CD4-FITC and the CD25-TR antibodies were applied to tissue slide. Likewise, the IL-10Rβ&TR-conjugated anti-goat IgG antibodies (1:500, Santa Cruz) and the CD4&FITC-conjugated anti-mouse IgG antibodies, and the CD161&FITC-conjugated anti-goat IgG antibodies (1:500, Santa Cruz) and the CD4&TR-conjugated anti-goat IgG antibodies (1:500, Santa Cruz) were used for the IL-10Rβ&CD4 and the CD161&CD4 double IHC stains, respectively.

### Statistical analysis

All data presented are the mean ± SD, and significant differences between two group and among the groups were determined by unpaired student's *t*-test and one-way ANOVA Fischer's PLSD post hoc test, respectively, using Stat View software (SAS Institute, Cary, NC).

## RESULTS

### Hepatic histological observation

FIGURE 1 SHOWS the hepatic histological observations from 0–8 weeks after T cells injection (G0, G2, G4, and G8) by H&E staining. Infiltration of inflammatory cells including mononuclear cells into the hepatic tissue were observed in the portal region of the hepatic lobule in G2 (Fig. 1b), consistent with our previous studies,[2–5] while these infiltrations were not observed in G0 (Fig. 1a). In the hepatic tissues, there were no other histological changes including necrosis, fatty change, and fibrosis in any of the GVHR mice, however, some cells that show the juvenile characters including enlarged form, strangely shaped nucleus, and faint colored cytoplasm were observed in the hepatic lesion through G2 to G8 (Fig. 1e). The infiltrations of inflammatory cells were gradually and significantly reduced over time and up to G8 (Fig. 1c–d, Fig. 2). The quantified area of infiltrated inflammatory cell was significantly decreased in G8 compared to that in G2 and G4 (Fig. 2). Similarly, the numbers of region with inflammatory cells per hepatic tissue area were significantly lower in G8 compared with G2 (Fig. 2). Under these conditions, there were no notable inflammatory regions or histological alterations in other tissues examined, including spleen, lung, heart, kidneys, and bone marrow between G0 and G2 to G8 groups (Data not shown).

### IHC stain

In the hepatic regions of infiltrated inflammatory cells, all examined markers (CD4, CD8, CD20, CD25, CD45ro, CD161, Foxp3, IL-10Rβ) were detectable by IHC stain at G2 (Fig. 3). These surface markers were also detectable in G4 to G8 but not in G0 (data not shown). Certain of the surface markers including CD25, CD4, CD161 and IL-10Rβ were studied by immunofluorescence in the liver at G2 (Fig. 4). Colocalization between CD25&CD4, IL-10Rβ&CD4, CD161&CD4 were clearly detected and all positive cells expressing both CD25 and IL-10Rβ also expressed CD4, while not all the CD161 positive cells expressed CD4 (Fig. 4).

Figure 5 presents the ratio of the cells that were positive for the specific surface marker to the total infiltrated inflammatory cells at G2 to G8. With the exception of the cells expressing IL-10Rβ, which presented similar level of expression from G2 to G8, all the other cells showed a significantly decreased expression at G4 and G8 vs. G2. Among the other organs studied, all the surface markers in the spleen and only CD20 in the bone marrow were detectable through G2 to G8 (Data not shown).

### Anti IL-10 antibody injected GVHR model

Pre-treatment of anti-IL-10 mAb with the GVHR mice significantly increased in the hepatic infiltration of inflammatory cells compared with that in the control IgG mAb-received GVHR mice (Fig. 6a,b). These findings are in agreement with our previous report.[5] However, in the IL-10-mAb-received GVHR mice, there was no detectable positive cell for IL-10Rβ in the infiltrated regions as measured by IHC staining (Fig. 6c). On the other hand, the expression level of Foxp3 was significantly enhanced by approximately 40% throughout the infiltrated region in the IL-10mAb-injected GVHR mice when compared to that in the control IgG

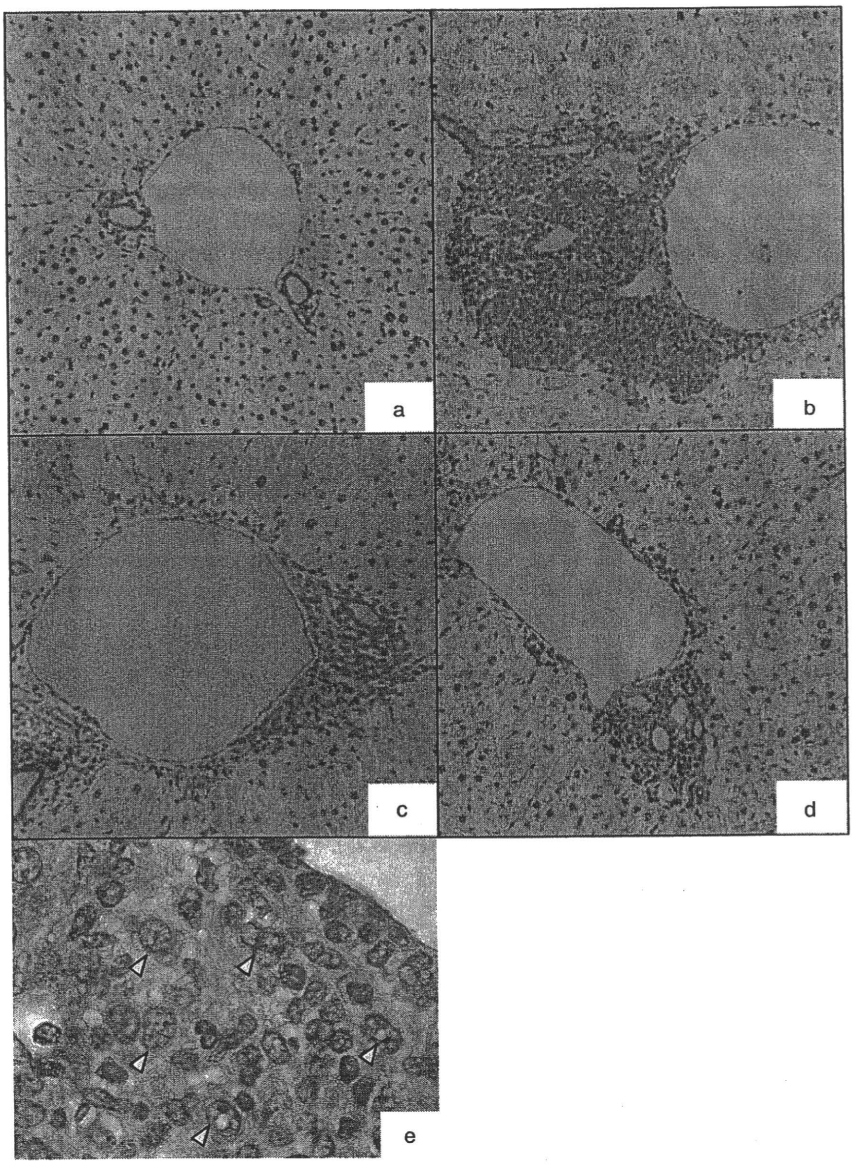


**Figure 1** Hepatic histological observations of infiltrated inflammatory cells in the graft versus host response (GVHR) mice by haematoxylin and eosin stain. The triangle arrows in Fig. 1e show the cells with juvenile characters. (a) GVHR at 0 week (× 25). (b) GVHR at 2 weeks (× 25). (c) GVHR at 4 weeks (× 25). (d) GVHR at 8 weeks (× 25). (e) GVHR at 2 weeks (× 100).

mAb-receiving mice (Figs 6d,7). In the IHC stains, there were no differences in the profiles of infiltrated lymphocytes against all examined surface markers between the G2 mice without anti-IL10mAb and the control IgG mAb-injected mice.

## DISCUSSION

THE PRESENT STUDY investigated the immune-related pathogenesis of hepatic inflammation throughout an 8-week period following injection of graft spleen T cells in the recipient mice. The hepatic infiltration of inflammatory cells reached a peak at

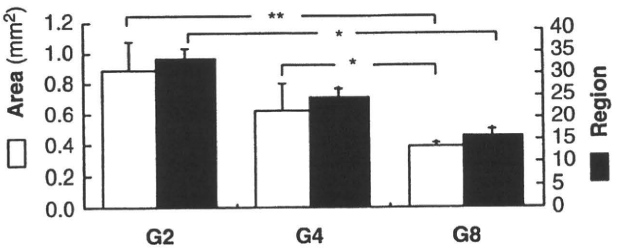


**Figure 2** Area and number of regions with infiltrated inflammatory cells in the hepatic tissue. G2, graft versus host response (GVHR) mice at 2 weeks; G4, GVHR at 4 weeks; G8, GVHR at 8 weeks. Data are presented as the mean ± SD. $*P < 0.05$; $**P < 0.01$ by one way ANOVA Fischer's PLSD post hoc test.

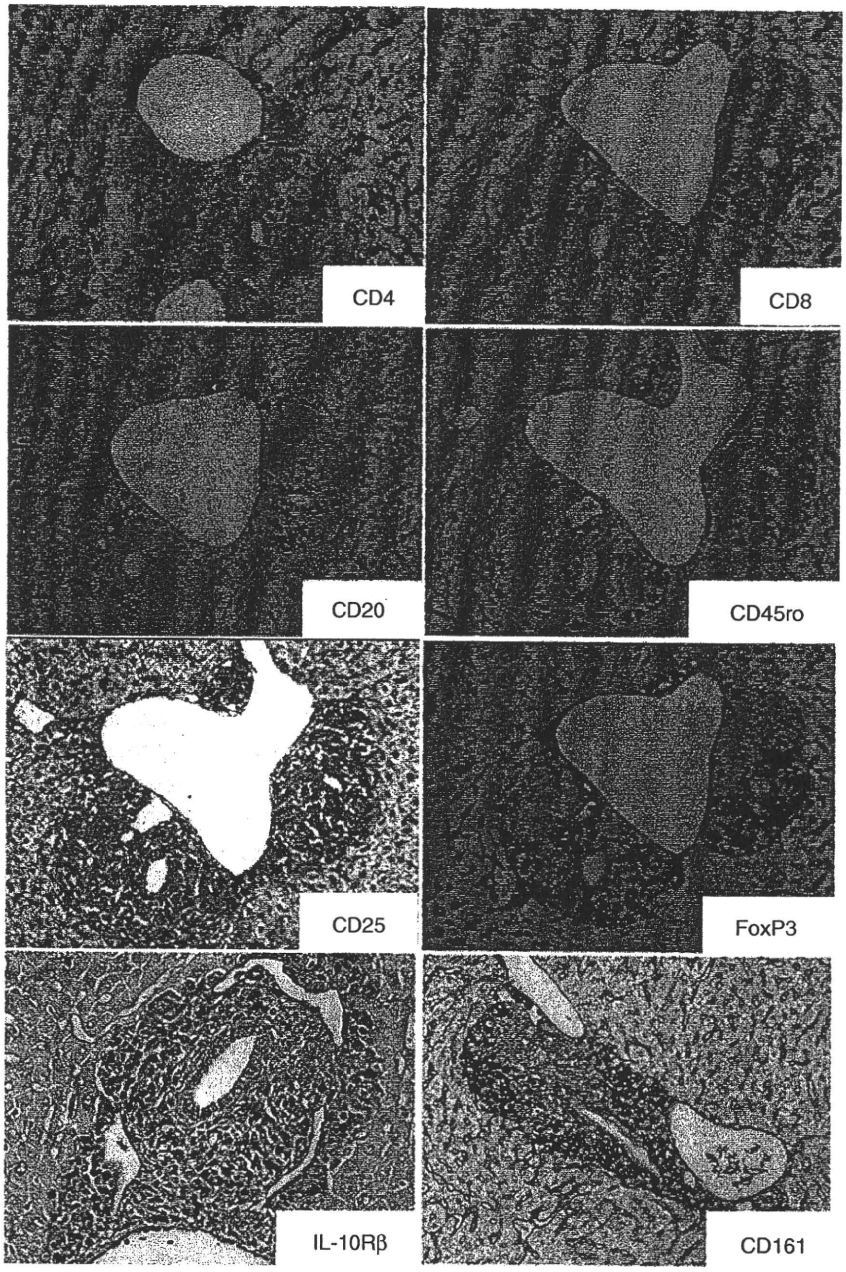


**Figure 3** Hepatic immunohistochemical stained images of various surface markers of infiltrated inflammatory cells in G2 (× 50).

2 weeks after the T cells transfer, as observed in our previous studies,[2–5] and gradually improved over the 8 weeks period studied. This progressive recovery from hepatic inflammation was a characteristic of the GVHR model mice, and clarifications of the mechanism(s) responsible for this recovery would have useful clinical impact for patients with immune-related liver diseases.

As preliminary experiment of this GVHR model, we analyzed comprehensive gene expressions of inflammatory-related cytokines in hepatic tissues infiltrated with inflammatory cells in G0, G2, and G8 by comparison of same age normal control without the T cells transfer using Panorama® Mouse Cytokine Gene array (Sigma). Among the genes that transiently increased at G2 and thereafter reduced at G8 along with the alteration of liver pathology, the highest expressed gene at G2 was IL-2Rγ that is one of three IL-2R subsets, α, β, and γ. The IL-2Rα is also named CD25 and is a

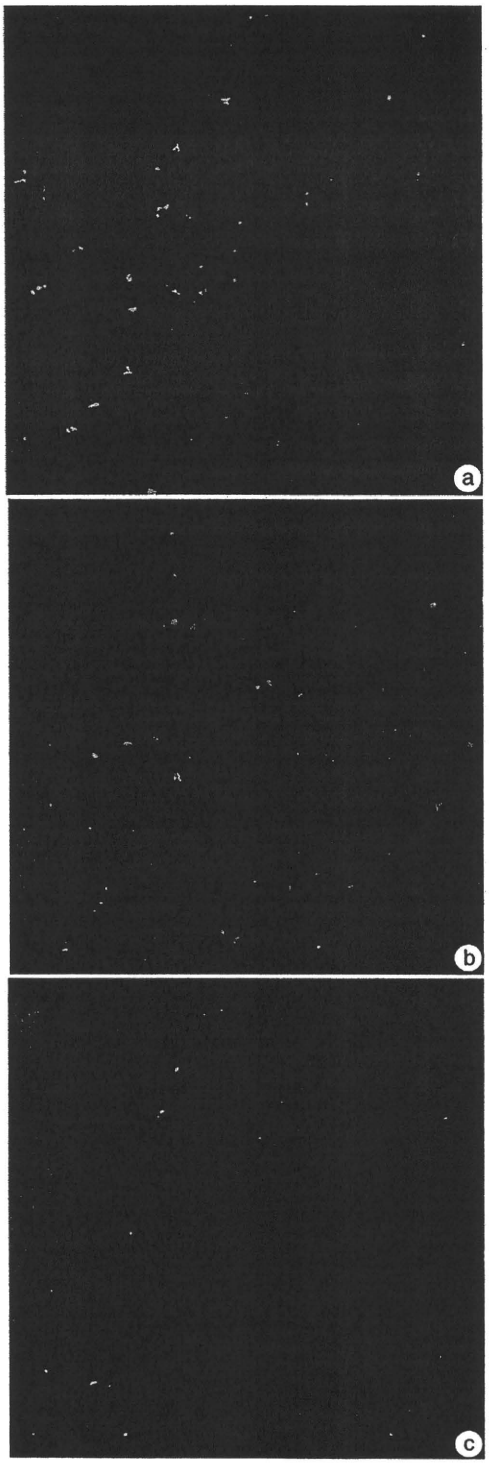


**Figure 4** Merged fluorescence immunohistochemical observations of the surface markers for the regulatory T (Treg) cells in hepatic tissue of graft versus host response (GVHR) mice at 2 weeks. (a) $CD4^+$(FITC) $CD25^+$(TR) Treg cells. (b) $CD4^+$(FITC) $IL10R\beta^+$(TR) cells. (c) $CD4^+$(TR) $CD161^+$(FITC) cells. (× 60) TR, Texas Red.

specific surface marker of $CD4^+CD25^+$Treg cells, while the other two subsets are actual receptors for IL-2.[19] Based on these findings, we focused the present study on the influence of Treg cells including $CD4^+CD25^+$Treg cells, Tr1 cells, and NKT cells on the hepatic inflammation in the GVHR mouse model.

The Treg cells are subsets of $CD4^+$ T cells that are negative regulators in the immune responses. Among these cells, $CD4^+CD25^+$Treg cells and IL-10 producing Tr1 cells are the best-characterized Treg cells,[12] and NKT cells also behave as the Treg cells. The $CD4^+CD25^+$Treg cells were recognized by the co-expressing of CD4 and CD25 or the expression of master gene; FoxP3.[12] The Tr1 and NKT cells also have specific surface marker of IL-10R and CD161, respectively.[10,12,20]

Specific markers of Treg cells were detectable in the infiltrated inflammatory cells in the hepatic tissue from G2 to G8. These findings show the infiltration of the Treg cells into the inflammation region of the liver together with other lymphocytes. Furthermore, the ratio of the $IL\text{-}10R\beta^+$ cells (Tr1 cells) to the total infiltrated cells remained over the 8 weeks, while most of the other markers studied, including CD4, CD8, CD20, CD45ro, CD25, CD161, and FoxP3, were only transiently elevated with a significant reduction at 8 weeks along with the recovery in inflammation.

Previously, we have demonstrated that the injection of anti-IL-10 mAb into GVHR mice prior to that of the spleen T cells dramatically enhanced the hepatic infiltration of inflammatory cells after 2 weeks.[5] It has been previously reported that the IL-10 could decrease hepatotoxicity in several animal models[21–27] and ameliorate the inflammation of human HCV hepatitis.[28,29] Groux *et al.* have reported that the Tr1 cells with inflammatory properties produced high levels of IL-10.[30] In the present study, the expression level of the Tr1 cells was not detectable in the hepatic infiltration region of inflammatory cells in the anti-IL-10mAb injected GVHR mice, while this was detectable for up to 8 weeks in the GVHR mice that did not receive any anti-IL-10 mAb injection. This difference in the expression suggests that the anti-IL-10 mAb might be responsible for the loss of Tr1 cell expression in the hepatic inflammatory region, which would be compatible with the report that the Tr1 cells are activated by IL-10.[30,31] In the cDNA macroarray of the preliminary analysis, the gene expression levels of IL-10 and TGF-β elevated at G2 and maintained at G8 without anti-IL-10 mAb (data not shown). Interestingly, the expression of Foxp3, a master gene for the $CD4^+CD25^+$Treg cells, in the hepatic infiltration region was dramatically enhanced in the anti-IL-10mAb

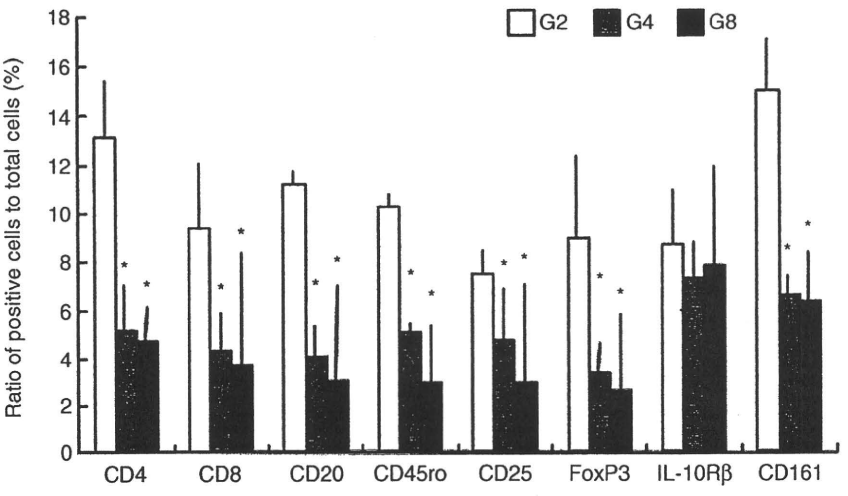


Figure 5 The ratio of the positive cells with the respective surface marker to the total infiltrated inflammatory cells in G2. The numbers of the positive cells and total cells were counted in the immunohistochemical and haematoxylin and eosin stained sections, respectively. G2, graft versus host response (GVHR) at 2 weeks; G4, GVHR at 4 weeks; G8, GVHR at 8 weeks. Data are presented as the mean ± SD. $^*P < 0.05$ compared to G2 by one way ANOVA Fischer's PLSD post hoc test.

injected GVHR mice after 2 weeks assessed by IHC. The $CD4^+CD25^+$Treg cells and the Tr1 cells belong to the same subset of Treg cells at different stages of differentiation, and both Treg cells have an interactive relationship on their respective activations and functions.[10] The $CD4^+CD25^+$Treg cells typically differentiate in the thymus,[19] while the Tr1 cells differentiate in the periphery from native precursors, typically in the presences of IL-10 as well as TGF-β.[30,31] The $CD4^+CD25^+$Treg cells may contribute to the differentiation of the Tr1 cells by producing both IL-10 and TGF-β[32–34] and the activated Tr1 cells also produce IL-10 and TGF-β as autocrine factors.[31] In the observation on H&E stain, some undifferentiated and juvenile cells of lymphocytes were observed in the inflammatory region of hepatic tissue in the GVHR mice (Fig. 1e). Therefore, we hypothesized that the Tr1 cells were recruited as a native precursors into the hepatic lesion, and thereafter, were differentiated at the lesion influenced by the $CD4^+CD25^+$Treg cells. The immunologic reaction in the hepatic tissue receded after a transient inflammation at 2 weeks by expression of Treg cells, particularly in Tr1 cells. There is a possibility that the time lag between the transient inflammation and subsequent recovery might be due to

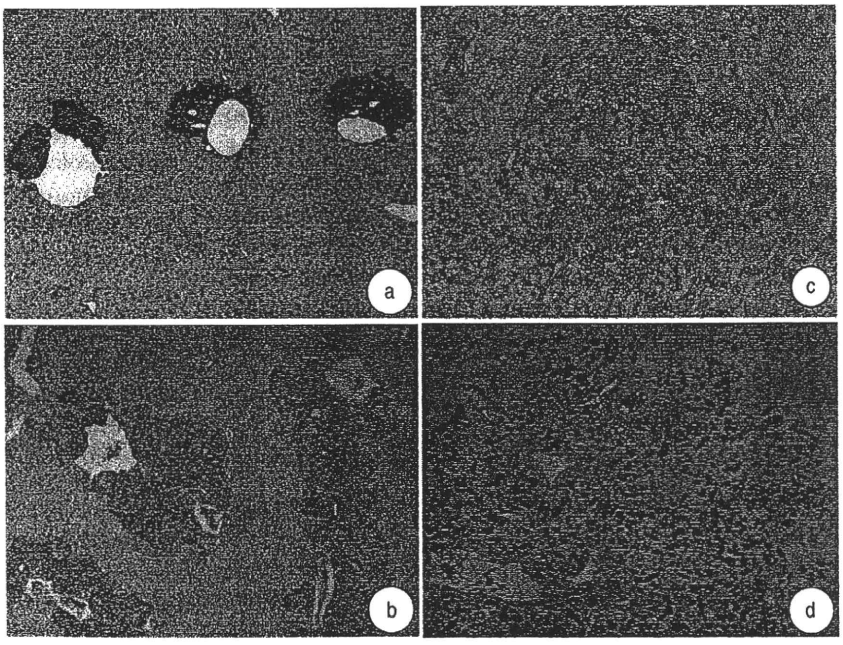


Figure 6 Histological observation of hepatic tissue from graft versus host response (GVHR) mice that were pretreated with the anti-IL-10 mAb. (a) Haematoxylin and eosin (H&E) image of GVHR mice liver that received the control mAb (× 13.5). (b) H&E image in GVHR mice liver that received the anti-IL-10 mAb (× 13.5). (c) Immunohistochemical (IHC) image for IL-10Rβ in GVHR mice that received the anti-IL-10 mAb (× 50). (d) IHC image for Foxp3 in GVHR mice that received the anti-IL-10 mAb (× 50).

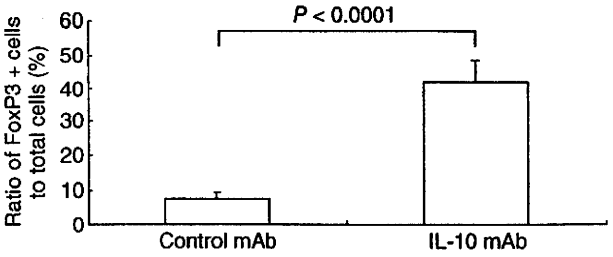


Figure 7 The ratio of positive cells with FoxP3 to the total hepatic infiltrated Inflammatory cells in the anti-IL-10 vs. control IgG mAb-injected mice after 2 weeks. Data are shown as the mean ± SD, and statistically analyzed by unpaired Student's *t*-test. mAB, monoclonal antibody.

the response time for down-regulation by the Tr1 cells after its differentiation in a peripheral site, i.e. in the infiltration site of hepatic tissue, by interaction with $CD4^+CD25^+$Treg cells. In our previous study, the expression of IFN-γ mRNA was elevated as early as 3 days after the spleen T cell injection. By contrast, the expression of the IL-10 mRNA was delayed by 2 weeks when the hepatic inflammation was at its maximum.[2] In the present study, the later expression of IL-10 mRNA after 2 weeks suggest that the recovery step of hepatic inflammation had already begun through the activation of Tr1 cells as a result of the enhanced IL-10 production.

$CD4^+CD25^+$Treg cells have been suggested to control their regulatory function by enhancing the differentiation of the Tr1 cells.[10] Dieckmann *et al.* have shown that the induction of the Tr1 cells *in vitro* by the $CD4^+CD25^+$Treg cells was mediated by cell-cell contact using human $CD4^+CD25^+$Treg cells or by the action of the $CD4^+CD25^+$Treg cells on antigen-presenting cells.[32] Based on the previous findings, the increased expression of Foxp3 in the anti-IL-10mAb injected GVHR mice could be the result of a compensatory or feedback mechanism and the inhibition of the Tr1 cells by anti-IL-10 mAb. Therefore, the findings of the present study lead us to the hypothesis that the Tr1 cells, but not the $CD4^+CD25^+$Treg cells, might directly down-regulate the immunologic response against the hepatic inflammation in the GVHR mice, and however, the $CD4^+CD25^+$Treg cells should be needed to differentiate the the Tr1 cells at the inflammatory sites.

In our previous study, the aggravation of the hepatic inflammatory response in the GVHR mouse model was also induced by concanavalin A (ConA),[4] similarly to the observed effect of anti-IL-10 mAb administration.[5] It has been reported that ConA suppressed the activation and/or proliferation of the $CD4^+CD25^+$Treg cells in the thymus and tonsil.[35,36] These data imply that the pathology of the GVHR model might be aggravated by suppression of either $CD4^+CD25^+$Treg cells or Tr1 cells. In other words, both $CD4^+CD25^+$Treg and Tr1 cells could be necessary for immune tolerance in the GVHR model. However, this hypothesis will need the further confirmation and investigation in the ConA-injected GVHR model.

The NKT cells are $CD4^+$ T cells that express the specific surface marker (CD161) of natural killer cells, and play the role of regulation in immunologic reaction by producing of IL-4 and IFN-γ.[20] Many studies have reported that NKT cells were selectively decreased in model mice and in patients with immune diseases.[37–39] In the present study, although many $CD161^+$ cells were detected in the hepatic inflammatory regions, the cells significantly decreased at G4 and G8 after the transient increase at G2. Furthermore, most of the $CD161^+$ cells did not co-express $CD4^+$ in the fluorescence IHC observation suggesting that the specifically CD161 positive cells are the natural killer cells. In addition, it has been reported that the positive selection in development of NKT cells requires the MHC class I-like molecule, CD1d.[20] On the other hand, the GVHR in the present study was caused by the differences in MHC class II.[7] Therefore, in the GVHR mice, the NKT cells might not be related with the recovery of immunologic response.

In conclusion, the findings of the present study support, at least partially, the expression and activity of the Treg cells as key factors in the induction of immune tolerance in GVHR liver diseases.

## ACKNOWLEDGEMENT

A PART OF this study was presented at The 19th The Meeting of Liver and Immunology, The 5th Japan Society of Hepatology Single Topic Conference, The 42nd Annual meeting of Japan Society of Hepatology, and The 107th Annual Meeting of the American Association for the Study of Liver Diseases and the Digestive Disease Week.

The authors also thank the Laboratory Animal Resource Center at the University of Tsukuba for their assistance with the breeding of the experimental animals.

T. Miyazaki and M. Doy contributed equally to this work.

## REFERENCES

1 Saitoh T, Fujiwara M, Asakura H. L3t4+ t cells induce hepatic lesions resembling primary biliary cirrhosis in mice

with graft-versus-host reactions due to major histocompatibility complex class II disparity. *Clin Immunol Immunopathol* 1991; 59: 449–61.
2 Itoh S, Matsuzaki Y, Kimura T *et al.* Cytokine profile of liver-infiltrating CD4+ T cells separated from murine primary biliary cirrhosis-like hepatic lesions induced by graft-versus-host reaction. *J Gastroenterol Hepatol* 2000; 15: 443–51.
3 Itoh S, Matsuzaki Y, Kimura T *et al.* Suppression of hepatic lesions in a murine graft-versus-host reaction by antibodies against adhesion molecules. *J Hepatol* 2000; 32: 587–95.
4 Unno R, Matsuzaki Y, Itoh S, Doy M, Shoda J, Tanaka N. Novel murine autoimmune-mediated liver disease model induced by graft-versus-host reaction and concanavalin A. *J Gastroenterol Hepatol* 2001; 16: 1149–57.
5 Unno R, Matsuzaki Y, Itoh S, Doy M, Shoda J, Tanaka N. Progression of autoimmune-mediated hepatic lesions in a murine graft-versus-host reaction by neutralizing IL-10. *Hepatol Res* 2003; 26: 354–61.
6 Van der Veen F, Rolink AG, Gleichmann E. Diseases caused by reactions of T lymphocytes to incompatible structures of the major histocompatibility complex. IV. Autoantibodies to nuclear antigens. *Clin Exp Immunol* 1981; 46: 589–96.
7 Ikarashi Y, Matsumoto Y, Omata S, Fujiwara M. Recipient-derived T cells participate in autoimmune-like hepatic lesions induced by graft-versus-host reaction. *Autoimmunity* 1995; 20: 121–7.
8 Toubi E Targeting T regulatory cells in autoimmune diseases. *Isr Med Assoc J* 2008; 10: 73–6.
9 Toubi E. The Role of CD4+CD25+ T Regulatory Cells in Autoimmune Diseases. *Clin Rev Allergy Immunol* 2008; 34: 338–44.
10 Veldman C, Nagel A, Hertl M Type I regulatory T cells in autoimmunity and inflammatory diseases. *Int Arch Allergy Immunol* 2006; 140: 174–83.
11 Sakaguchi S. Naturally arising Foxp3-expressing CD25+CD4+ regulatory T cells in immunological tolerance to self and non-self. *Nat Immunol* 2005; 6: 345–52.
12 Thompson C, Powrie F. Regulatory T cells. *Curr Opin Pharmacol* 2004; 4: 408–14.
13 Jiang H, Chess L. An integrated view of suppressor T cell subsets in immunoregulation. *J Clin Invest* 2004; 114: 1198–208.
14 Saitoh T, Ikarashi Y, Ito S, Watanabe H, Fujiwara M, Asakura H. Depletion of CD8+ cells exacerbates organ-specific autoimmune diseases induced by CD4+ T cells in semiallogeneic hosts with MHC class II disparity. *J Immunol* 1990; 145: 3268–75.
15 Hori S, Nomura T, Sakaguchi S. Control of regulatory T cell development by the transcription factor Foxp3. *Science* 2003; 299: 1057–61.
16 Khattri R, Cox T, Yasayko SA, Ramsdell F. An essential role for Scurfin in CD4+CD25+ T regulatory cells. *Nat Immunol* 2003; 4: 337–42.
17 Fontenot JD, Gavin MA, Rudensky AY. Foxp3 programs the development and function of CD4+CD25+ regulatory T cells. *Nat Immunol* 2003; 4: 330–6.
18 Powrie F, Maloy KJ. Immunology regulating the regulators. *Science* 2003; 299: 1030–1.
19 Jordan MS, Boesteanu A, Reed AJ *et al.* Thymic selection of CD4+CD25+ regulatory T cells induced by an agonist self-peptide. *Nat Immunol* 2001; 2: 301–6.
20 Seino KI, Fukao K, Muramoto K *et al.* Requirement for natural killer T (NKT) cells in the induction of allograft tolerance. *Proc Natl Acad Sci USA* 2001; 98: 2577–81.
21 Arai T, Hiromatsu K, Kobayashi N *et al.* IL-10 is involved in the protective effect of dibutyryl cyclic adenosine monophosphate on endotoxin-induced inflammatory liver injury. *J Immunol* 1995; 155: 5743–9.
22 Louis H, Le Moine O, Peny MO *et al.* Hepatoprotective role of interleukin 10 in galactosamine/lipopolysaccharide mouse liver injury. *Gastroenterology* 1997; 112: 935–42.
23 Louis H, Le Moine O, Peny MO *et al.* Production and role of interleukin-10 in concanavalin A-induced hepatitis in mice. *Hepatology* 1997; 25: 1382–9.
24 Louis H, Van Laethem JL, Wu W *et al.* Interleukin-10 controls neutrophilic infiltration, hepatocyte proliferation, and liver fibrosis induced by carbon tetrachloride in mice. *Hepatology* 1998; 28: 1607–15.
25 Thompson K, Maltby J, Fallowfield J, McAulay M, Millward-Sadler H, Sheron N. Interleukin-10 expression and function in experimental murine liver inflammation and fibrosis. *Hepatology* 1998; 28: 1597–606.
26 Nagaki M, Tanaka M, Sugiyama A, Ohnishi H, Moriwaki H. Interleukin-10 inhibits hepatic injury and tumor necrosis factor-alpha and interferon-gamma mRNA expression induced by staphylococcal enterotoxin B or lipopolysaccharide in galactosamine-sensitized mice. *J Hepatol* 1999; 31: 815–24.
27 Yoshidome H, Kato A, Edwards MJ, Lentsch AB. Interleukin-10 suppresses hepatic ischemia/reperfusion injury in mice: implications of a central role for nuclear factor kappaB. *Hepatology* 1999; 30: 203–8.
28 Nelson DR, Lauwers GY, Lau JY, Davis GL. Interleukin 10 treatment reduces fibrosis in patients with chronic hepatitis C: a pilot trial of interferon nonresponders. *Gastroenterology* 2000; 118: 655–60.
29 Nelson DR, Tu Z, Soldevila-Pico C *et al.* Long-term interleukin 10 therapy in chronic hepatitis C patients has a proviral and anti-inflammatory effect. *Hepatology* 2003; 38: 859–68.
30 Groux H, O'Garra A, Bigler M *et al.* A CD4+ T-cell subset inhibits antigen-specific T-cell responses and prevents colitis. *Nature* 1997; 389: 737–42.
31 Roncarolo MG, Bacchetta R, Bordignon C, Narula S, Levings MK. Type 1 T regulatory cells. *Immunol Rev* 2001; 182: 68–79.
32 Dieckmann D, Bruett CH, Ploettner H, Lutz MB, Schuler G. Human CD4(+)CD25(+) regulatory, contact-dependent